2004-11-29

Pluton Zonation Unveiled by Gamma-ray Spectrometry and Magnetic Susceptibility; A Case Study of the Sheeprock Granite, Western, Utah

Paul D. Richardson
Brigham Young University - Provo

PLUTON ZONATION UNVEILED BY GAMMA RAY SPECTROMETRY AND MAGNETIC SUSCEPTIBILITY: THE SHEEPROCK GRANITE, WESTERN, UTAH

by

Paul Douglas Richardson

A thesis submitted to the faculty of

Brigham Young University

in partial fulfillment of the requirements for the degree of

Master of Science

Department of Geology

Brigham Young University

December 2004

BRIGHAM YOUNG UNIVERSITY

GRADUATE COMMITTEE APPROVAL

of a thesis submitted by
Paul Douglas Richardson

This thesis has been read by each member of the following graduate committee and by majority vote has been found to be satisfactory.

_____	_____
Date	Eric H. Christiansen, Chair
_____	_____
Date	Bart J. Kowallis
_____	_____
Date	Mike J. Dorais

BRIGHAM YOUNG UNIVERSITY

As chair of the candidate's graduate committee, I have read the thesis of Paul D. Richardson in its final form and have found that (1) its format, citations, and bibliographical style are consistent and acceptable and fulfill university and department style requirements; (2) its illustrative materials including figures, tables, and charts are in place; and (3) the final manuscript is satisfactory to the graduate committee and is ready for submission to the university library.

_____
Date

_____
Eric H. Christiansen
Chair, Graduate Committee

Accepted for the Department

_____
Bart J. Kowallis
Graduate Coordinator

Accepted for College

_____
Gale Bryce
Dean, College of Physical and Mathematical Science

ABSTRACT

PLUTON ZONATION UNVEILED BY GAMMA-RAY SPECTROMETRY
AND MAGNETIC SUSCEPTIBILITY:
THE SHEEPROCK GRANITE,
WESTERN, UTAH

Paul Douglas Richardson

Department of Geology

Master of Science

A radiometric survey of the zoned 21 Ma, A-type Sheeprock granite, western Utah, combined with measurements of magnetic susceptibility and field observations were analyzed using a geographic information system. The intrusion spans 25 km^2 and is roughly elliptical in shape with its long axis trending northwest. Concentration maps (composed of more than 500 survey stations) of eU, eTh, texture, magnetic susceptibility, color, and joint density help to constrain magmatic and post-magmatic processes related to its chemical and physical zonation. Uranium ranges from 3.9 to 26.9 ppm (mean 12.7) and thorium from 1.7 to 125.7 ppm (mean 45.5). Similarities in spatial patterns and near normal distributions of U and Th imply minimal remobilization and secular equilibrium of U.

Relatively high magnetic susceptibility (6 to $12*10^{-3}$ SI units), low eU and eTh, and limited whole rock chemical analyses show the southeastern part of the pluton is more mafic and most likely formed as an early cumulate. Dominant textures are porphyritic with a fine-grained matrix along the northeastern margin, coarsening to a

medium-grained matrix along the southwestern margin. This transition from fine to medium-grained matrix textures is believed to be a preserved solidification front that had migrated from the roof and walls inward during cooling. Late stage magma mixing is evidenced by a string of mafic enclaves along the axis of the pluton near this solidification front. eU and eTh generally increase toward the finer-grained northeastern margin of the pluton. This has been interpret this to be primarily the result of fractionation of U and Th into monazite and thorite. As mafic cumulates formed along the northeastern margin residual liquids were displaced inward. This depleted the more evolved parts of the pluton in U and Th. Beryl, a distinguishing characteristic of the most evolved portions of the pluton, is concentrated in two areas along the central axis of the intrusion. The intrusion is a cumulative of three magmatic phases, the second of which crystallized from the margins inward.

Joint spacing is a major factor in controlling post-magmatic processes. The pluton has a higher density of joints (10 cm apart) near the upper margins, and fewer joints (> 1 meter apart) at lower elevations. Differential cooling and magma pressures are believed to have controlled the varying joint densities. Increased alteration, oxidation, and red-staining are more prevalent in areas of higher joint density. Magnetic susceptibility is bimodal. The high mode ($5.4 * 10^{-3}$ SI) is on the low end of magnetite-series granites and occurs most often in white granites. The low mode ($0.07 * 10^{-3}$ SI) implies significant post-magmatic oxidation and the destruction of magnetite and correlates to red granite. Truncated chemical and textural patterns along the pluton's northwestern margin support evidence for range front normal faulting.

ACKNOWLEDGMENTS

A work of this magnitude is never wrought about individually. I would like to express my sincere appreciation to those who have aided me along the way. Thanks to the BYU geology department for the use of their vehicles. My committee chairman Dr. Christiansen; this paper would have never reached its full potential had it not been for his helpful reviews and insightful discussions. Thanks to those who helped me in my field work: Greg Melton, Lonnie Mercer, Dave Tingey, and my brothers Steve and Michael Richardson. I am grateful to my grandfather for the use of his camper and four wheeler and my uncle steak for lending me his 9mm pistol and the piece of mind it brought to me in cougar country. Special thanks to my parents who supported me from start to finish. And my wife Jenny, without her love and support I may have never finished.

TABLE OF CONTENTS

LIST OF TABLES

LIST OF FIGURES

INTRODUCTION

To understand intrusive rocks, their cooling and crystallization histories, mechanics of intrusion, and overall geochemical evolution, many factors must be considered. The nature and origin of zonation in granites are key aspects that must be understood. Some major questions about pluton zonation concern its internal and external geometries. What do the shapes of internal boundaries in the pluton tell us about its cooling history? Are they chemical or textural in nature? Are internal contacts intrusive surges or steep geochemical "slopes" caused by differentiation? Is the zonation gradational or sharp, systematic or patchy? Do variations in texture correspond with internal chemical contacts, assimilation, or cumulates? Is chemical and textural zonation a result of in situ crystal fractionation or of progressive injection of an evolving melt? To answer these questions a detailed understanding of compositional patterns is required. However, getting enough data to create a detailed chemical map of a pluton by traditional methods of collecting samples and laboratory analysis is difficult, time consuming, and expensive.

This is a case study using the Sheeprock granite, a chemically zoned pluton in western Utah (Christiansen et al., 1988). We re-examined the zonation of this pluton in more detail by measuring variations in K_2O, eU, eTh, and magnetic susceptibility using a portable gamma-ray spectrometer and a magnetic susceptibility meter. Potassium, uranium, and thorium are sensitive to magmatic fractionation and gamma-ray spectrometry provides a method of conveniently and rapidly measuring compositional changes over large areas of rough terrain (Thorpe, 1995; Chiozzi et al., 1998). Magnetic

susceptibility can be linked to the oxygen fugacity and the total Fe in rocks, which declines with differentiation in granitic magmas (Gleizes et al., 1993). Using these data, combined with careful field observations, we have attained a new level of understanding its chemical zonation and other aspects of its magmatic and post-magmatic evolution.

GEOLOGIC SETTING

The Sheeprock Mountains lie about 90 km southwest of Salt Lake City, Utah, in the Basin and Range province (Figure 1). A small granite pluton outcrops on the southwestern flank of the Sheeprock horst and covers 25 km^2. The prominent white cliffs, rugged topography, and high relief of the Sheeprock granite combined with its joint-controlled crags and cliffs stand in contrast to the sedimentary and metasedimentary rocks it intrudes. The intrusion is roughly elliptical in shape, with its long axis oriented northwest. The pluton is nearly continuously exposed except for exposures in the bottom of Joes Canyon and two other isolated outcrops to the southeast.

The granite is a white, light gray to pinkish porphyritic rock with a fine to coarse-grained matrix. Many exposures exhibit intense iron staining (resulting from the oxidation of magnetite and pyrite to hematite and limonite) that follows, but is not limited to fractures, giving the rock a banded appearance in many places.

The 21 Ma Sheeprock granite is contemporaneous with aluminous, A-type rhyolites erupted during the late Cenozoic and related to bimodal volcanism and lithospheric extension that created the Basin and Range province (Christiansen et al., 1988). Like the rhyolites, the Sheeprock granite contains trace amounts of topaz and is enriched in Be, U, Th, Rb, Ta, F, and other rare elements. There is no clear evidence that

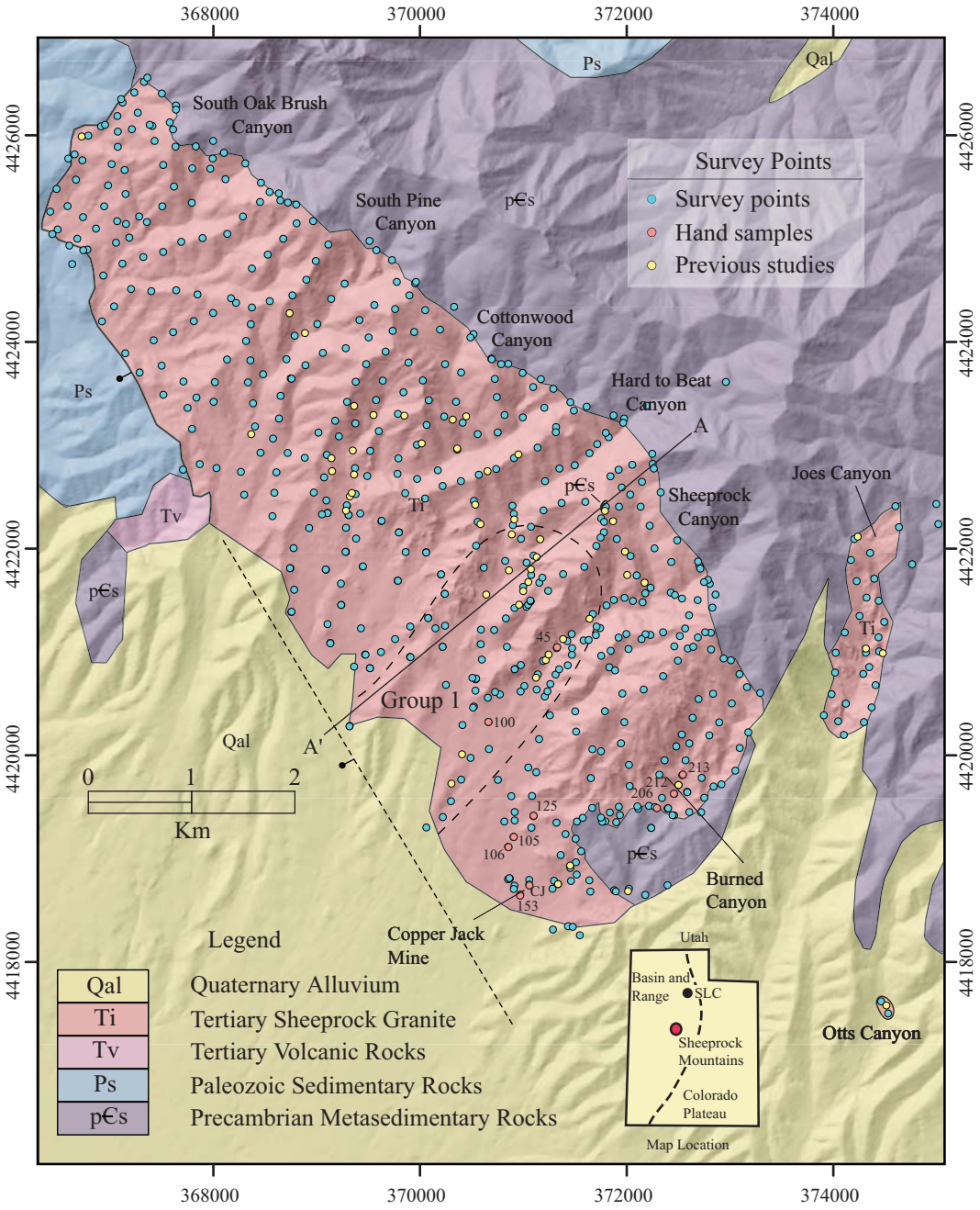

Figure 1. Geologic map of the Sheeprock granite witht he locations of survey stations and samples. Coordinates in UTM. SLC = Salt Lake City on inset map of Utah. Simplified geology after Panpeyan (1989). Group 1, delineated by Christiansen et al., (1988) represents the highly evolved core, and is based on a small set of labratory samples.

depletions of compatible elements suggest the granite core is highly differentiated (Christiansen et al., 1988). Beryl rosettes are characteristic of this part of the pluton (Rogers, 1990). Group 2 samples are from the pluton's marginal zone and were thought to be similar in composition to the parent magma. Group 3 rocks were interpreted to be mafic cumulates that formed along the chamber margins, displacing residual liquids inward. Groups 2 and 3 do not have a distinct distribution and are intermingled, making interpretations difficult.

Faulting

The pluton intrudes folded and faulted late Proterozoic quartzites, slates, phyllites, and diamictites along its northeastern and southern margins, and is in fault contact with Paleozoic carbonate rocks in the northwest (Figure 1). Paleozoic sedimentary rocks along the north and northwestern margins of the pluton (consisting of quartzite, limestone, and dolomite) comprise the hanging wall. Based on the regional dips of these rocks sedimentary rocks contacting the Sheeprock granite are stratigraphically out of place and unconformably lower in section. These units are rotated and brecciated along the margin of the pluton and lack any evidence of contact metamorphism expected along contacts with carbonate rocks. NW-trending normal faults have been identified in mines near the mouth of South Oak Brush canyon and are referred to by Cohenour (1959) as being part of a "Western Flank fault zone". A small exposure of a middle Tertiary ignimbrite near South Pine Canyon is probably in fault contact with the Sheeprock granite. Although portions of the pluton's southwestern margin are covered by Cenozoic alluvium, there is evidence of a continuation of these

the Sheeprock chamber ever erupted to the surface (Cohenour, 1959). The depth of emplacement is difficult to establish from field evidence, but normative feldspar compositions plot below the two kb cotectic (Whitney, 1975), suggesting a shallow depth.

Mineralogy

Mineral assemblages in the Sheeprock granite are typified by phenocrysts of K-feldspar (1-4 cm in maximum dimensions) and quartz. Quartz, Na-plagioclase, K-feldspar, Fe-rich biotite, fluorite, ilmenite, and magnetite make up the matrix. Accessory minerals include topaz (contained in vugs and some phenocrysts), zircon, apatite, U-Th-rich monazite, Nb-Ta oxides, thorite, xenotime, and rare uraninite (Funkhouser-Marloff, 1985). Blue beryl can be found as disseminated crystals (2 mm or less), unique rosette structures (from 3 to 50 cm in diameter), and in small veinlets (Rogers, 1990).

Zonation

Early mapping of the pluton separated the granite into two facies-- a white core facies, and a red facies, characterized by its limonite staining (Cohenour, 1959). Whole rock compositions also show the pluton to be chemically zoned. Christiansen et al., (1988) divided the pluton into three chemical groups: Group 1 consisted of the strongly differentiated samples from the core as outlined in Figure 1. This area is texturally varied and enriched in Rb, Y, Na, F, Sc, Be, Li, and other incompatible elements, and depleted in LREE (light rare earth elements), Fe, Mg, Ca, K, Sr, Ba, U, Ti and P. U and Th, which are generally considered incompatible are also depleted in the Group 1 rocks (Funkhouser-Marlof, 1985). The high concentrations of incompatible elements and

NW-trending faults from the north (e.g., spring occurrences and geomorphic features) and is referred to by Cohenour (1959) as the "South Flank fault".

TECHNIQUES

Previous studies of the chemical zonation of the Sheeprock granite were based on a limited number (~20) of analyzed laboratory samples. They lacked adequate sample density and distribution to reveal chemical variations across the entire pluton accurately (Figure 1). A more detailed and systematic study of compositional variations, combined with pertinent field observations, has created higher resolution maps more accurately representing the chemical and physical zonation of the pluton.

Data Collection

Field data and geographic locations for survey stations and sample sites were recorded using a Trimble GeoExplorer III global positioning system (GPS). At each site, total radiometric response, K_2O, eU, eTh, magnetic susceptibility, texture, the presence or absence of beryl, color of granite, and joint spacing were measured and recorded. In addition, dikes, greisen alteration, veins, enclaves, and xenoliths were also noted.

A total of 600 measurements were made in granite and country rock over a period of 36 days. Grid sampling of the pluton was impractical because of the uneven distribution of outcrops. Survey points were spaced about 200-300 meters apart (concentrated on the ridges and in the canyons) and distributed as uniformly as possible throughout the pluton (Figure 1).

Samples were collected from ten sites: nine granites and one mafic enclave

(Figure 1). A water-cooled, gas-powered core drill equipped with a 1" diamond-tipped bit was used to collect about a kilogram of rock to be used for X-ray fluorescence analysis (XRF).

X-ray Fluorescence Sample Preparation and Analysis

To calibrate the gamma-ray spectrometer, granite samples were analyzed by X-ray fluorescence to determine major and trace element concentrations. Samples were powdered using a tungsten carbide shatter box and dried overnight in an oven at 105°C. For major element analyses, glass disks were prepared by fusing rock powder with a 50/50 mixture of lithium tetraborate and lithium metaborate flux. Analytical surfaces of the fused disks were then polished with 1000 grit silica carbide. For trace element analysis, rock powders were pressed into pellets backed by Whatman fibrous cellulose powder. Major and trace element concentrations were determined using a Siemens SRS-303 X-ray fluorescence spectrometer. Results of XRF analyses and the analytical precision of our instrument compared with a known international reference standard (NIMG) are shown in Table 1.

Radiometric Survey

Because of the high U and Th concentrations in the Sheeprock granite, a portable gamma-ray spectrometer provided a method of rapidly assaying concentrations, in outcrop, at a large number of localities (Cassidy, 1981). The survey was carried out using a portable Scintrex GRS-500 gamma-ray spectrometer. The instrument assigns gamma-ray energies associated with the decay of ^{40}K (1.35 to 1.59 Mev) to potassium, ^{214}Bi (1.65 to 1.87 Mev) to uranium, ^{208}Tl (2.45 to 2.79 Mev) to thorium. Total

Table 1. Major and trace element analyses of granite from the Sheeprock pluton, Utah.

Sample ID	SR-213	SR-206	SR-CJ	SR-153	SR-106	SR-105	SR-125	SR-100	SR-45	SR-212*	Standard NIMG		
Easting	372539	372400	371057	370969	370851	370906	371097	370662	371323	372459	Acc.	Avg.	Std. Dev.
Northing	4419808	4419488	4418795	4418652	4419115	4419210	4419412	4420323	4421038	4419626		n = 2	
					Oxide wt.%								
SiO_2	73.79	75.48	72.33	76.44	74.74	75.09	76.02	75.60	77.79	62.07	75.70	75.80	0.16
TiO_2	0.20	0.18	0.25	0.10	0.23	0.14	0.15	0.12	0.10	1.22	0.09	0.09	0.00
Al_2O_3	13.78	13.18	14.30	13.02	13.35	13.35	12.66	13.13	12.08	17.35	12.08	12.11	0.06
Fe_2O_3	1.52	1.23	2.29	0.90	1.79	1.26	1.26	1.09	1.18	6.16	2.02	2.05	0.00
MnO	0.03	0.03	0.06	0.03	0.06	0.05	0.03	0.02	0.03	0.17	0.02	0.02	0.00
MgO	0.23	0.18	0.66	0.12	0.23	0.15	0.16	0.14	0.13	1.47	0.06	0.08	0.01
CaO	0.85	0.62	1.87	1.00	0.78	0.86	0.99	1.08	0.57	2.42	0.78	0.78	0.01
Na_2O	3.43	3.41	3.45	3.53	3.75	3.74	3.56	3.72	3.79	4.99	3.36	3.28	0.01
K_2O	6.09	5.65	4.72	4.86	5.00	5.32	5.13	5.05	4.30	3.69	4.99	4.99	0.01
P_2O_5	0.07	0.03	0.07	nd	0.07	0.04	0.05	0.05	0.02	0.47	0.01	0.04	0.01
Total	100.00	100.00	100.00	100.00	100.00	100.00	100.00	100.00	100.00	100.00			
LOI	0.57	0.40	0.44	0.63	0.55	0.61	0.70	0.84	0.53	1.24	0.59	0.59	0.00
Anal. Total	99.74	99.61	100.08	100.81	100.26	98.82	100.79	99.93	99.78	99.47	99.70	99.81	0.23
					Trace element abundance (ppm)								
F	646	2579	1166	416	3742	2714	1829	1644	5146	5529	4200	4203	4.9
Cl	35	100	46	48	22	5	nd	16	nd	460	400	217	3.3
Sc	nd	nd	5	nd	nd	nd	nd	nd	nd	15	1	0	0.0
V	9	9	29	5	4	2	3	5	13	29	2	2	2.3
Cr	2	2	5	nd	2	1	3	4	1	2	12	11	0.0
Ni	1	1	2	nd	2	1	1	1	3	6	8	5	1.1
Cu	nd	nd	nd	nd	nd	nd	nd	nd	2	2	12	9	1.2
Zn	16	16	28	5	26	17	16	9	9	110	50	52	0.2
Ga	17	18	16	13	21	20	19	21	23	38	27	25	0.2
Rb	319	384	185	235	461	467	409	471	628	402	320	316	0.4
Sr	112	56	308	79	10	20	30	74	31	208	10	12	0.1
Y	15	29	12	8	56	54	39	17	69	101	143	134	11.2
Zr	156	159	100	64	215	171	138	98	140	389	300	287	2.5
Nb	40	54	22	18	137	133	63	64	143	232	53	50	1.2
Ba	370	189	858	242	251	145	175	194	80	411	120	118	4.0
La	50	92	25	22	71	52	48	25	54	64	109	134	22.3
Ce	90	124	65	48	132	92	103	67	78	173	195	188	2.1
Nd	33	41	26	nd	50	35	40	27	30	83	72	67	5.3
Sm	8	11	5	6	12	9	10	7	8	15	16	17	0.1
Pb	9	12	15	21	16	18	14	17	23	9	40	40	1.6
Th	29	73	10	22	83	85	73	49	77	36	51	57	0.8
U	7	12	5	5	16	16	14	14	26	12	15	13	0.1
					Gamma-ray spectrometery								
K_20 wt%	4.4	5.4	4.3	4.8	5.7	5.3	5.3	5.6	4.4				
eU ppm	9.6	15.7	3.9	4.6	11.6	18.0	17.3	13.5	19.7				
eTh ppm	46.0	65.4	10.4	16.6	69.6	77.9	66.4	77.9	67.7				
					Magnetic Susceptibility								
$MS*10^{-3}$	7.7	0.2	10.7	5.6	6.3	6.2	6.2	5.1	0.6				
Color	white	white	banded	white	banded	banded	white	white	white				
Joints	1 m	1 m	> 1 m	10 cm	> 1 m	> 1 m	1 m	1 m	1 m				

1. Normalized to 100% on a volatile free basis
2. An. Total = analytical total
3. LOI = loss on ignition at 1000ºC for 4 hours
4. nd = not detected
5. * = mafic enclave
6. MS = magnetic susceptibility
7. Acc. = accepted
8. Avg. = average
9. Std. Dev. = standard deviation

radiometric response is assessed by processing all gamma-rays with energies above 400 Kev. To take into account short term instrumental drift caused by temperature variations, the calibration was adjusted in the field using an external ^{113}Ba reference source. Measurements were recorded in counts per second (cps). The spectrometer was placed directly against the rock, on outcrops that were generally flat and unaltered, although iron staining was unavoidable in some places.

Six measurements, with ten second sampling periods, were averaged at each survey station. This minimum number of analyses was determined by calculating a running average of 10 repeat measurements on a granite slab measuring 76 x 36 x 40 cm (Figure 2). Lab results on this slab gave averages of 65.1 ± 2.4 cps for total radiometric response, 6.1 ± 0.7 cps for potassium, 1.5 ± 0.4 cps for uranium, and 0.5 ± 0.2 cps for thorium (Table 2). Tests conducted in the field gave similar if not better precision because of higher concentrations of U and Th in the Sheeprock granite. Field uncertainties represent an average of 12 six-count measurements conducted over a period of 3 days in different locations.

To convert gamma-ray spectrometer measurements into concentrations, calibrations lines were constructed by regressing counts per second (cps) as measured on outcrops in the field versus XRF-derived concentrations for rocks collected from those outcrops. An comparison of the two techniques is shown in Figure 3. A simple linear regression was used to convert Th cps to eTh ppm (1) and multi-linear regressions were used for eU (to account for overlap in the Th channel) (2), and for K_2O (to account for overlap from U and Th)(3).

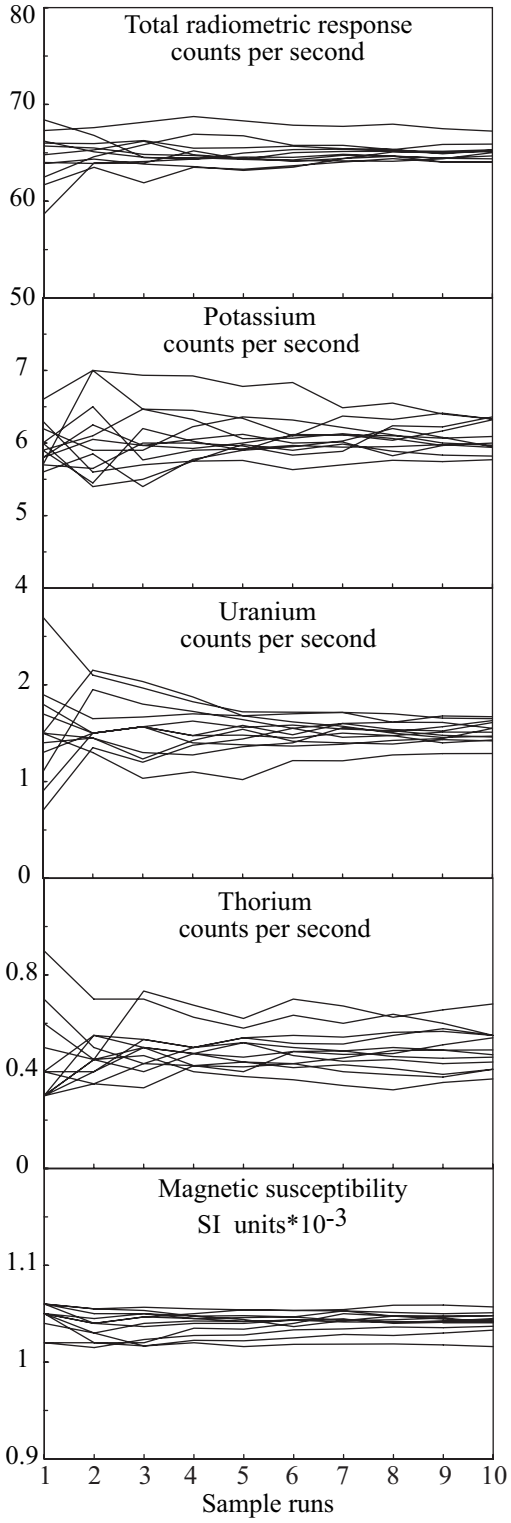

Figure 2. Running averges used to determine the minimum number of measurements needed per station using the gamma-ray spectrometer and magnetic susceptibility meter. In each case an average of six measurements was adequate in representing the rock.

Table 2. Precision estimates for gamma-ray spectrometry and magnetic susceptibility data

	Lab Analysis			Field Analysis		
	Mean	Std. Dev.	% Dev.	Range	Std. Dev.	% Dev.
TRR cps	65.1	2.4	3.8	128-184	3.7	2.1
K cps	6.1	0.7	11.8	10-16	0.9	7.2
U cps	1.5	0.4	29.9	4-7	0.7	13.7
Th cps	0.5	0.2	39.1	1-3	0.6	25.6
Mag SI	1.0	0.02	1.5	0-5	0.3	35.0

1. Field analysis precision calculated from reproducibility at 12 different locations
2. TRR = Total radiometric response
3. Mag SI = Magnetic susceptibility $*10^{-3}$ SI units

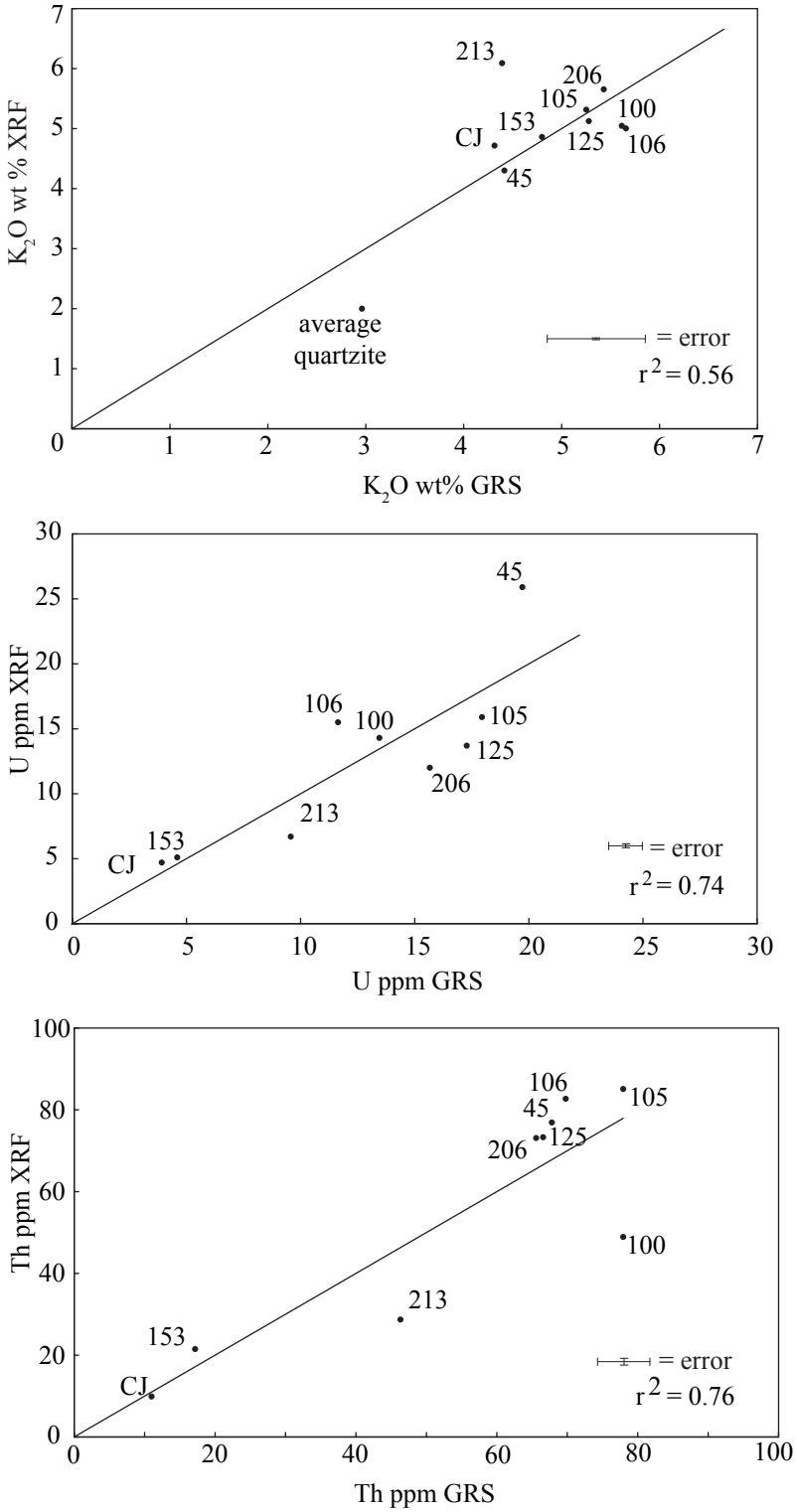

Figure 3. The correlation between X-ray fluorescence (XRF) concentrations and those calculated by gamma-ray spectrometry (GRS).

$$\text{eTh ppm} = 24.888 * Th\ cps - 11.238 \quad (1)$$

$$r^2 = 0.76$$

$$\text{eU ppm} = [(U\ cps * 2.998327) + (Th\ cps * -1.60496) + -0.29022] \quad (2)$$

$$r^2 = 0.74$$

$$K_2O\ \text{wt\%} = [(K\ cps * 0.848133) + (U\ cps * -1.18617) + (Th\ cps * -0.357733) + 1.840723] \quad (3)$$

$$r^2 = 0.56$$

Uranium and thorium concentrations were within the ranges of existing data for the Sheeprock granite. However, about 36% of the gamma-ray spectrometry analyses of K_2O were greater than 6 wt% and higher than most granites (Figure 4).

Of the 527 original measurement sites in granite, about 40% of the Th analyses had to be rejected because of instrument malfunction. Potassium concentrations for these anomalous sites were corrected by revisiting a small set of locations and regressing "old" against "new" data. U and total radiometric response were unaffected by the instrument problem and all analyses were used. Because of the uneven distribution of valid Th concentrations, greater degrees of interpolation were needed to create this map.

Magnetic Susceptibility Survey

Magnetic susceptibility was measured using a Micro KAPPA Field Rock Magnetic Susceptibility Meter model KT-5, to see how changes in magnetic susceptibility correlated with chemical and textural zonation. The instrument measures both true and apparent susceptibility. However, at susceptibilities lower than $100*10^{-3}$ SI units, true susceptibility = apparent susceptibility with an error of less than 5%. Measurements were recorded in $SI*10^{-3}$ units and corrected for surface unevenness. Variations in magnetic susceptibility correspond to concentrations of magnetite, thus

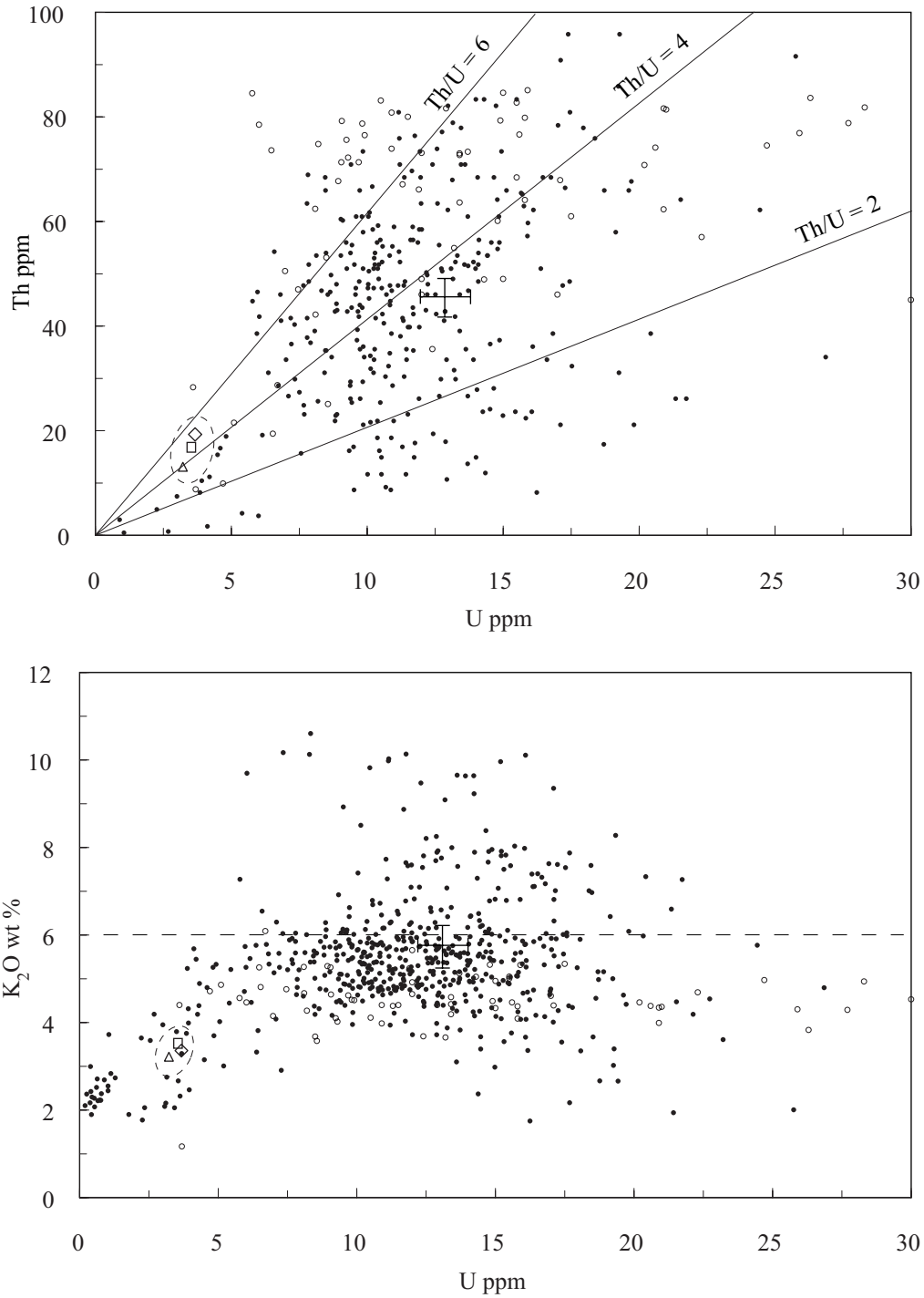

Figure 4. K, U, and Th concentrations derived by gamma-ray spectrometry of outcrops (small closed circles) and X-ray fluorescence spectrometry of collected samples (open cirlces). Average granite (open square), average peraluminous granite (open diamond) and average metaluminous granite (open triangle) compositions for the United States (Stuckless et al., 1982). Means (± 1 std. dev.) of gamma-ray spectrometer data are shown with a cross.

equal intervals. Specific variables for each map are summarized in Appendix A.

Radioelements

Total radiometric response varies from 60 to 292 cps with a mean value of 164 cps (Table 3). A histogram of the total radiometric response shows a near normal distribution with the mean and median near the mode (Figure 5). The map (Figure 6a) shows lows (<120 cps) in the southwest grading to higher values (>200 cps) to the northeast with contours following the long axis of the pluton. Lower count rates are more prominent in the lower elevations (Figure 7c) of the pluton, while highs are more concentrated along the upper ridges and peaks. A steep geochemical gradient exists in the southeastern corner of the pluton near the Copper Jack mine, where the total radiometric response drops from 190 to 100 cps in less than 500 meters.

Of the three radio elements studied, potassium is the most problematic. Due to the extremely long half life of ^{40}K the gamma-ray spectrometer is relatively insensitive to ^{40}K even at 5-6 K_2O wt% levels. Data reduction is complex, because of U and Th overlaps and errors are much larger prohibiting proper quantitative analysis of K_2O variations (Figures 3 and 4). However, taken at face value K_2O varies from 1.8 to 10.6 wt% with a mean value of 5.6 wt% (Table 3). A histogram for K_2O shows a near normal distribution (Figure 5). Nevertheless, it is positively skewed more than any other variable as evidenced by abnormally high concentrations. It also has the highest kurtosis value suggesting many of these highs may be anomalous. K_2O wt% values for the Sheeprock granite are much higher than the 3.52 wt% average for granites of the contiguous United States (Stuckless and Van Trump, 1982) and may be the result of this

Table 3. Radiometric and magnetic susceptibility survey results

	TRR cps	K_2O wt%	eU ppm	eTh ppm	Th/U	Mag SI
Min	60.3	1.8	3.9	1.7	0.4	0.0
Max	292.3	10.6	26.9	125.7	8.8	12.7
Count	521	527	527	308	308	523
Mean	163.7	5.6	12.7	45.5	4.0	2.1
Std. Dev.	33.5	1.3	3.5	19.3	1.7	2.6
Median	160.1	5.5	12.5	46.0	4.0	0.7
Skewness	0.5	1.0	0.4	0.3	0.1	1.1
Kurtosis	4.1	5.3	3.9	3.3	2.7	3.4

1. TRR = total radiometric response
2. Mag = magnetic susceptibility*10^{-3} SI units

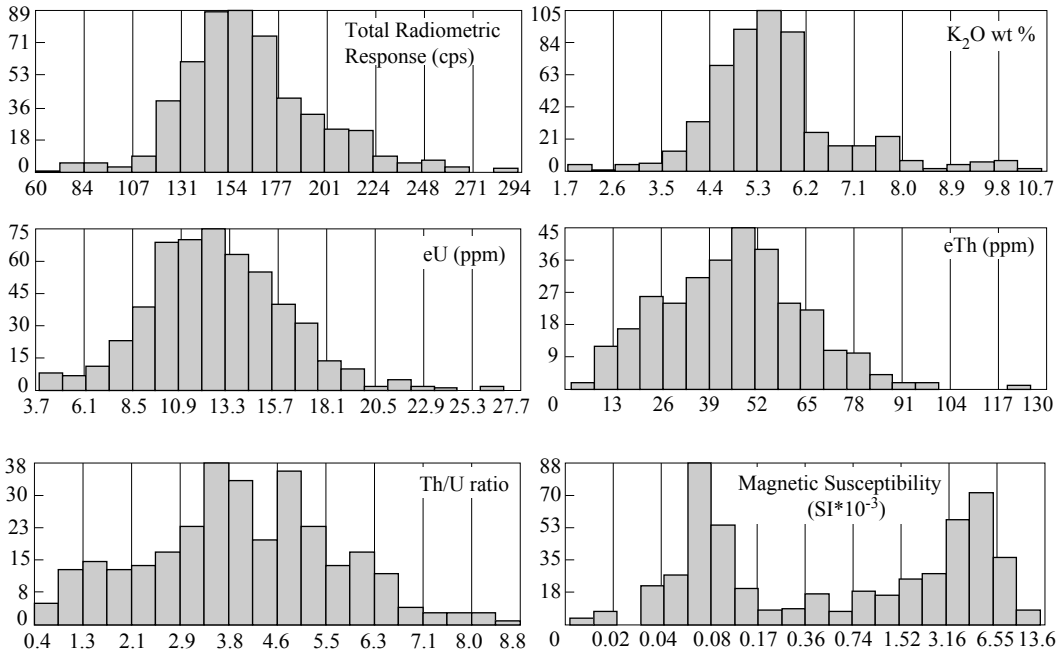

Figure 5. Radiometric and magnetic susceptibility data from the Sheeprock granite. All show near normal distributions, with the exception of magnetic susceptibility which under a log transformation shows a bimodal distribution.

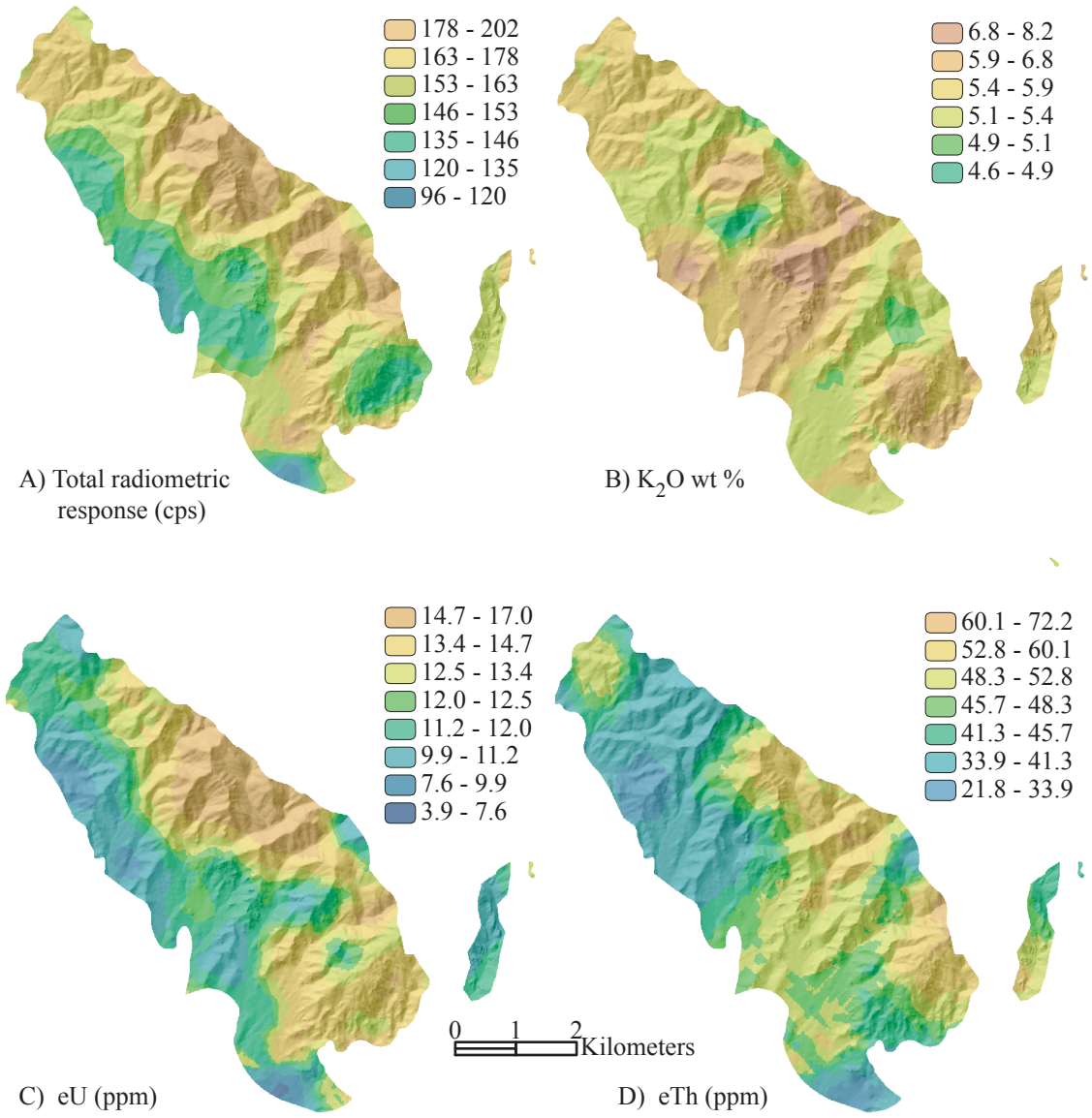

Figure 6. Variation maps of A) Total radiometric response, B) K_2O wt %, C) eU, and D) eTh.

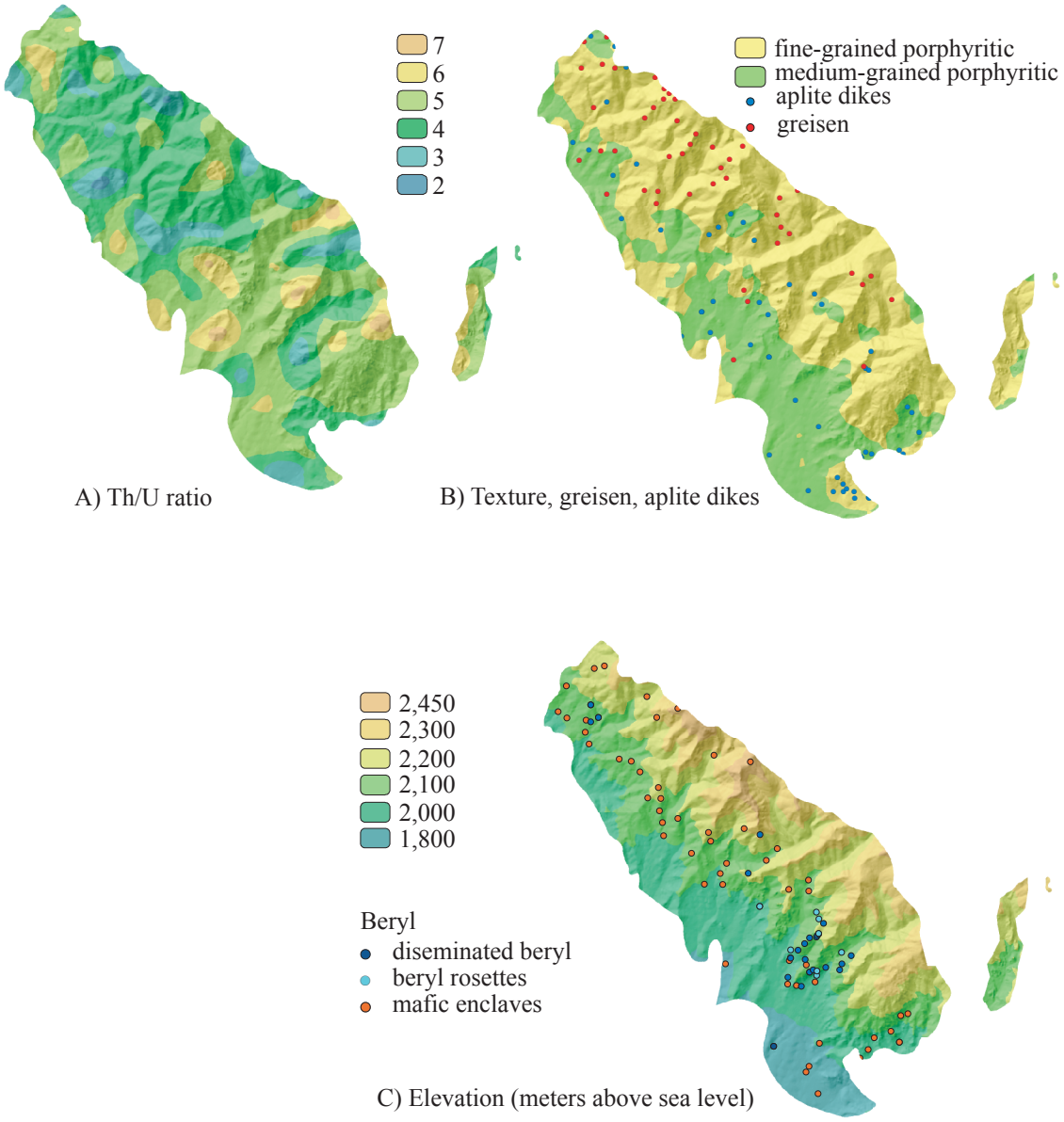

Figure 7. Maps of A) Th/U ratio, B) Texture (including aplite dikes and greisen), and C) Elevation (including beryl and mafic enclaves).

roughly representing mafic mineral concentrations in granite, which generally decline with differentiation (e.g., Gliezes et al., 1993).

Six measurements were needed to represent the rock effectively as judged from a running average of 10 repeat measurements conducted on a granite test slab (Figure 2). Analytical precision is summarized in Table 2. The greater variability of field measurements may be the result of surface irregularities and variable oxidation of rocks at individual outcrop measurements.

RESULTS

All field data were entered into a geographic information system (GIS)(ArcGIS 9.0) and analyzed for zonal patterns and relationships among the variables. Figure 5 shows histograms for each variable and Table 3 is a summary of the survey results. Included in Table 3 are the statistical variables skewness and kurtosis. Skewness is a measure of the symmetry of a distribution and equals zero for normal distributions. Kurtosis reflects the size of the tails of a distribution and provides a measure of how likely the data set will produce outliers. Kurtosis for a normal distribution is three. Maps (Figures 6, 7, and 8) were constructed by interpolating between areas of no data to create a continuous surface. Interpolated points were based on the proximity and similarity of nearby sample points using a maximum of 20 nearest neighbors (2 - 5 in each quadrant) and using kriging algorithms to predict values in areas of no data. Radiometric values were classified using a smart quantile classification, which tries to find a balance between highlighting changes in the middle and extreme values. A log transformation was used to help normalize the data for magnetic susceptibility. Other maps were contoured by

insensitivity (Figures 3 and 4). From the northwest to the southeast of the pluton, a pattern of alternating highs and lows appear (Figure 6b). A pronounced high runs northeast following the ridge between Hard to Beat and Cottonwood Canyons with a few other isolated highs in Burned and South Pine Canyons. Lows are found near the mouth of Cottonwood Canyon and around the upper fork in Sheeprock Canyon.

Uranium varies from 4 to 27 ppm (Table 3; Figure 4) with a mean value of 12.7 ppm compared with the continental granite average of 3.5 ppm (Stuckless and Van Trump, 1982). The histogram shows a near normal distribution (Figure 5). A slight positive skew and a relatively high kurtosis suggest some abnormality to the data set. Uranium concentrations grade upward to the northeastern intrusive margin with contours roughly following the long axis of the pluton and drop dramatically across the contact into metasedimentary rock (~2.6 ppm) (Figure 6c). Highs (> 15 ppm) are concentrated along the northeastern margin of the pluton and in the area between Sheeprock and Burned Canyons. Uranium lows are concentrated in the lower elevations along the southwestern margin of the pluton, with pronounced lows in areas south of South Oak Brush Canyon (9 - 6 ppm) and around the Copper Jack mine (< 5 ppm) in the southern tip of the pluton. A tongue of low uranium granite extends up from the mouth of Hard to Beat Canyon and over the ridge separating it from Sheeprock Canyon in the area where “Group 1" samples are concentrated (Figure 1).

Thorium varies from 2 to 126 ppm with a mean value of 46 ppm (Table 3, Figure 4) compared with the continental average of 16.8 ppm (Stuckless and Van Trump, 1982). A histogram of Th shows its near normal distribution with mean, median, and mode all

within one ppm. A kurtosis of 3.3 suggests these data are good with minimal outliers. Th distribution is similar to that of total radiometric response (Figure 6a) and U (Figure 6c) with the granite NE of the long axis of the pluton generally more enriched. There is also a prominent Th low (average of 11.5 ppm) in the granites of the Copper Jack mine area which can also be seen in maps of the total radiometric response and U. However, low Th values along the northern margin of the pluton and moderate values at the mouth of Hard to Beat canyon do not follow the pattern established by U. Like U, concentrations are distinctly lower in the adjacent country rock (~ 4.7 ppm).

The Th/U ratio varies widely from 0.4 to 8.8 (Table 3, Figure 4 and 5) but has a mean of 4.0, essentially the same as the continental granite average Th/U = 4.0 (Phair and Gottfried, 1964), Th/U = 4-5 (Peterman et al., 1981), and Th/U = 4.73 (Stuckeless and Van Trump, 1982). Variations of the Th/U ratio are more patchy than gradational (Figure 7a). Though not as obvious, areas of lower Th/U ratios are more common in the northern half of the pluton, from Cottonwood Canyon to South Oak Brush Canyon, with an exception of a high in the northwestern portion of the pluton that seems to correlate with local concentrations of beryl (Figure 7c). Areas of higher Th/U ratios are more concentrated in the half of the pluton from Hard to Beat Canyon south to Burned Canyon, with low ratios in the Copper Jack mine area.

Magnetic Susceptibility

Magnetic susceptibility ranges from 0.01 to $13*10^{-3}$ SI units (Table 3) with a mean of 2.1. However, a log-transformed histogram of the magnetic susceptibility shows a bimodal distribution (Figure 5); the lower mode is about $0.07*10^{-3}$ SI units and the

higher mode is about 5.4 $*10^{-3}$ SI units with only a few sites having magnetic susceptibilities between 0.17 and 0.74. Contours of the log transformed data follow the long axis of the pluton with granite of low susceptibility at higher elevations along the northeastern intrusive margin (Figure 8c). High susceptibilities are found along the southwestern margin and in the northwest near South Oak Brush Canyon. The granite in the Copper Jack mine area has the highest susceptibilities (> $10*10^{-3}$ SI). Magnetic susceptibility appears to be inversely correlated with total radiometric response, eU and eTh (Figures 6a, c, d, and 7c). A weakly positive correlation was found between magnetic susceptibility and Fe content in the Sheeprock granite (Figure 9).

Texture

The texture of the granite was mapped using nine categories: fine-, medium-, and coarse-grained equigranular; fine to medium, medium to coarse, and fine to coarse seriate; and porphyritic with fine, medium, and coarse-grained groundmass. Of these, the two dominant textures are porphyritic with a fine-grained matrix (grains < 2 mm) and porphyritic with a medium-grained matrix (grains 2-5 mm). Collectively, these two textures represent 90% of the sites. Because of the sparseness of other textures, only fine and medium-grained porphyritic textures are shown on the map (Figure 7b). The transition from fine to medium-grained porphyritic granite follows the long axis of the pluton dividing it roughly in half. Fine-grained matrices are most common along the northeastern intrusive contact with coarser rocks to the southwest. Nonetheless, in detail textures along the contact are often variable and can transition from chilled margins to phenocryst-rich and cumulate-like in less than 100 meters as observed in South Oak

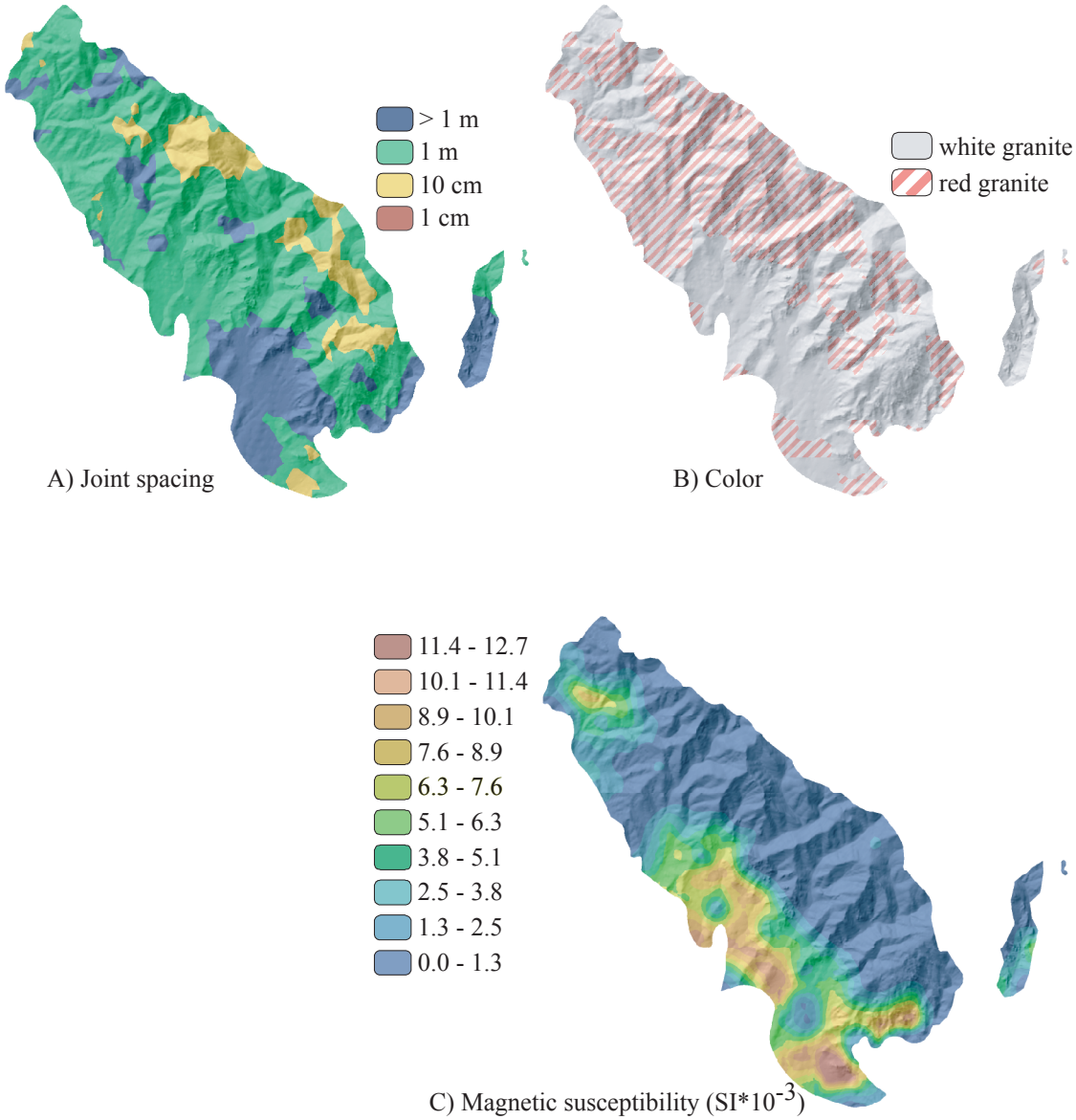

Figure 8. Concentration maps of A) Joint spacing, B) Color, and C) Magnetic susceptibility on a log transform basis.

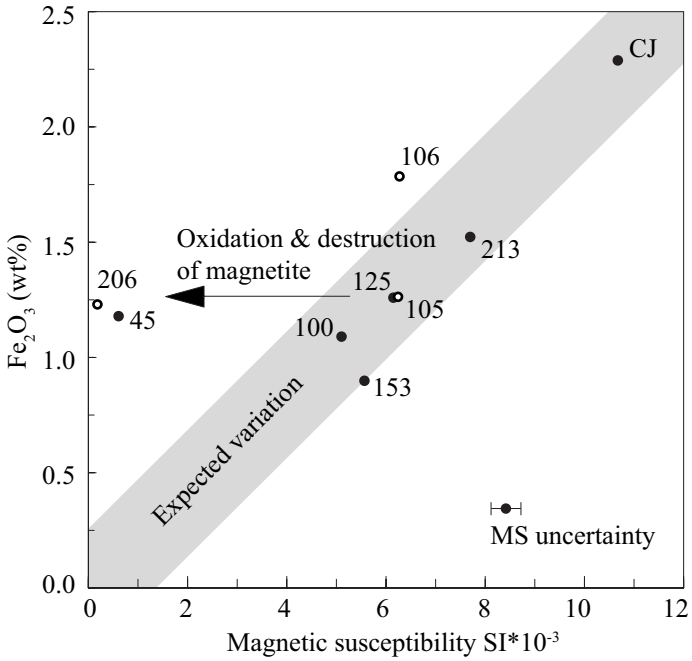

Figure 9. A weak positive correlation between Fe content and magnetic susceptibility may be complicated by variable destruction of magnetite during alteration and weathering. Open circles are banded granite, while closed circles are white granite outcrops. Samples 45 and 125 are located in banded areas. Expected variation is based on I-type granites from Blevin (2003).

Brush Canyon.

Beryl

Blue beryl is very rare in other granites, but occurs in several forms in the Sheeprock granite: disseminated crystals (≤ 2 mm) are most common, beryl rosettes (ranging from 3 to 50 cm in diameter), and in veins in order of abundance (Rogers, 1990). Beryl is concentrated in two areas (Figure 7c). The largest area is between Cottonwood Canyon and Sheeprock Canyon with the highest concentrations in Hard to Beat Canyon. A smaller grouping of beryl rosettes and disseminated crystals is located in the northern end of the pluton near the mouth of South Oak Brush Canyon. Htay (1976) showed beryl concentrations to be the most abundant between the elevations of 1,980-2,280 meters above sea level, very similar to our findings.

Xenoliths

Metasedimentary xenoliths derived from the wallrock occur along the northeastern margins of the pluton and in Burned Canyon near the contact. They range from fist-sized to a meter or more in diameter and are predominantly quartzite. Many of these xenoliths retain their original bedding structures. A large (~10 m x 40 m x 2 m) isolated xenolithic structure on the ridge between Hard to Beat and Sheeprock Canyons is interpreted to be a roof pendant and was mapped as undifferentiated Precambrian rocks by Cohenour (1959) (Figure 1). The pendant is blackish-brown, biotite-rich quartzite, and has low magnetic susceptibility ($1.1*10^{-3}$ SI) and higher than average U and Th (22 and 64 ppm) than the surrounding granite. A similar biotite-rich quartzite formed along the granite/country rock contact on the ridge between Sheeprock and Burned Canyons.

This contact is at about the same elevation as the described pendant.

Enclaves

The locations of approximately 60 mafic enclaves were recorded during the survey. Enclaves are more common along the long axis of the pluton (Figure 7c). This trend is parallel to the gradational chemical contours in the radiometric maps and magnetic susceptibility, and lies along the transition from fine to medium-grained textures (Figures 6a, c, d; 7b; 8c). It is worth mentioning that beryl appears to lie along this same trend. Enclaves range in size from less than 10 cm to greater than 1 meter in diameter and are in sharp contact with the granite. They are typically rounded to sub-rounded and contain megacrysts of euhedral alkali feldspar like those in the granite. Major minerals are plagioclase, K-feldspar, biotite, quartz, and oxides. Accessory minerals are euhedral apatite and subhedral titanite and epidote (possibly secondary). Quartz is undulose, and often appears to be secondary, and may have formed as the enclave equilibrated with the surrounding granite magma. Biotites are ragged and the only euhedral grains are apatite and oxides which are both abundant. Thin-section analysis shows two types of apatite, small equant crystals and accicular prisms. Unlike the granite there are no radiation haloes around inclusions in biotite. Based on one whole rock chemical analysis, enclaves are quartz monzonitic in composition (Table 1, sample 212). They are enriched in Al, Fe, Ti, Mg, Ca, Na, P and depleted in Si and K relative to the host granite. Enclaves have higher than average magnetic susceptibilities (5 to $11*10^{-3}$ SI) than the granite, because of abundant mafic mineral content, especially magnetite. On a normalized trace element diagram the enclave lacks the negative Nb

anomaly found in the granites (Figure 10). The enclave was slightly lower in U (12 ppm) and Th (36 ppm) than the average Sheeprock granite (13 ppm U and 46 ppm Th).

Dikes and Greisen

Both aplite dikes and greisen are common to the Sheeprock granite. Their orientations, densities, and spatial occurrences within the pluton are useful in understanding magmatic and post-magmatic processes. Aplite dikes are believed to represent late residual melts, while greisen veins are evidence for post-magmatic thermal alteration. Aplite dikes are the most abundant in the southwestern half of the pluton (Figure 7b). Dikes are more common in areas of medium-grained matrix textures. Greisen veins are more concentrated in the northeastern half of the pluton near the intrusive margin and in the northwestern portions of the Sheeprock granite.

Joint Spacing

The Sheeprock granite is strongly jointed and joint distribution may help interpret its cooling, alteration, and weathering history. Joints are typically steep and near vertical; some are sub-horizontal and probably formed by exfoliation (Harris, 1957; Cohenour, 1959). At each survey station, joint spacing was categorized as 1cm, 10 cm, 1 m, and >1 m. The most common spacing distance is 1 m (green), and can be found throughout the pluton (Figure 8a). Areas with joint spacings >1 m (blue) are concentrated in the low-lying parts of the granite along the southwestern flank of the pluton, and in the bottoms of some canyons. Areas with joint spacings ~10 cm (yellow) are fewer, and are concentrated along the northeastern side of the intrusion and wrap around to the southern contact, forming a discontinuous arc of moderate joint density.

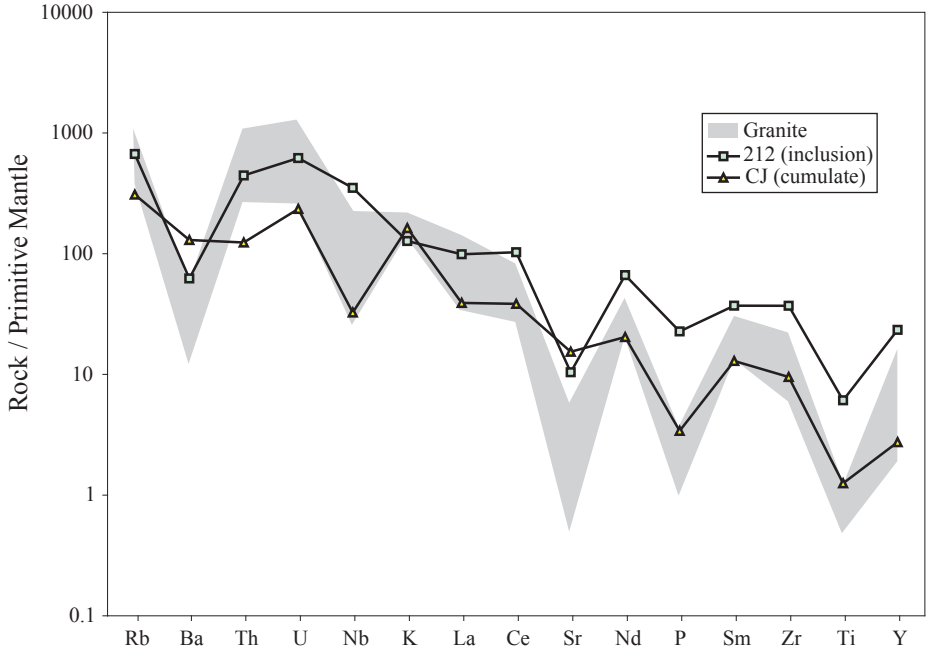

Figure 10. Trace element patterns for rocks from the Sheeprock pluton. Shaded area is the trace element range for 8 samples of granite. A mafic enclave (212) and the "mafic" sample from the Copper Jack mine (CJ) are shown separately. Normalization values from Sun and McDonough (1995).

This forms a crude concentric pattern of 10 cm spaced joints along the northeastern edge of the pluton with wider spaced joints toward the middle of the granite all in a "background" of joints spaced 1 m apart . This pattern is grossly similar to patterns seen on maps of total radiometric response, U, Th, and texture (Figures 6a, c, d; 7b).

Color

Previous studies divided the granite into zones based on color. A marginal red (limonite-stained) facies and core white facies (non-stained) were described by Harris (1957), Cohenour (1959), and Htay (1976). Although the distribution of red and white granite is systematic, no clear contacts were observed in the field. White granite is most common in the southwestern part of the intrusion (lower elevations) from the mouth of Cottonwood Canyon to Sheeprock Canyon and along the northern slope of Burned Canyon as well as a majority of Joes Canyon (Figure 8b). The area of white granite mapped in this study is strikingly similar to that mapped by Harris (1957) and strongly correlates with magnetic susceptibility concentrations (Figure 8c). Areas of joint spacing greater than or equal to 1 m typically correlate to white granite (Figure 8a). The remainder of the granite is iron-stained and banded. Severe jointing, red-banded color, and fine-grained textures along the northeastern margin of the pluton were also observed by Harris (1957).

DISCUSSION

In summary, field gamma ray spectrometry shows the Sheeprock granite is extremely enriched in U and Th compared to other granites. Moreover, the large data set shows the detailed geometry of the geochemical zonation. The radiometric survey shows

a gradation from lower concentrations of U and Th in the southwest along the partially covered margin (lower elevations) to higher concentrations in the northeast along the intrusive margin (higher elevations). High values are often associated with fine-grained porphyries, close joint spacing, low magnetic susceptibility, and red banding. The Copper Jack mine area (in the SE part of the pluton) has distinctively lower U and Th and high magnetic susceptibility. Magnetic susceptibility shows a bimodal distribution and and correlation to oxidation. Below, our interpretations are subdivided into magmatic and post-magmatic processes. See Figure 11 for a summary of correlations.

Magmatic Processes

The granite is principally composed of porphyritic rocks with fine-grained to medium-grained groundmasses (Figure 7b). The matrix texture is probably an indicator of cooling rate, which is a function of distance from the contact as described by Bachl et al., (2001) in a study of the Searchlight pluton, Nevada. The proximity of fine-grained matrix textures to the northeastern intrusive contact suggests more rapid cooling in this part of the intrusion, probably because it was closer to the roof or walls of the pluton (Harris, 1957). Medium-grained matrix textures suggest a slower cooling rate prevailed away from the margins. The transition from fine-grained porphyritic to medium-grained porphyritic textures may represent a preserved solidification front, as described by Bachl et al., (2001) for the Searchlight pluton, that propagated from the roof and margins inward during cooling (Figure 12a). This downward propagation of crystallization may have controlled the distribution of mafic enclaves and beryl and will be discussed in greater detail later in the text. Based on the assumption that the pluton's textures formed

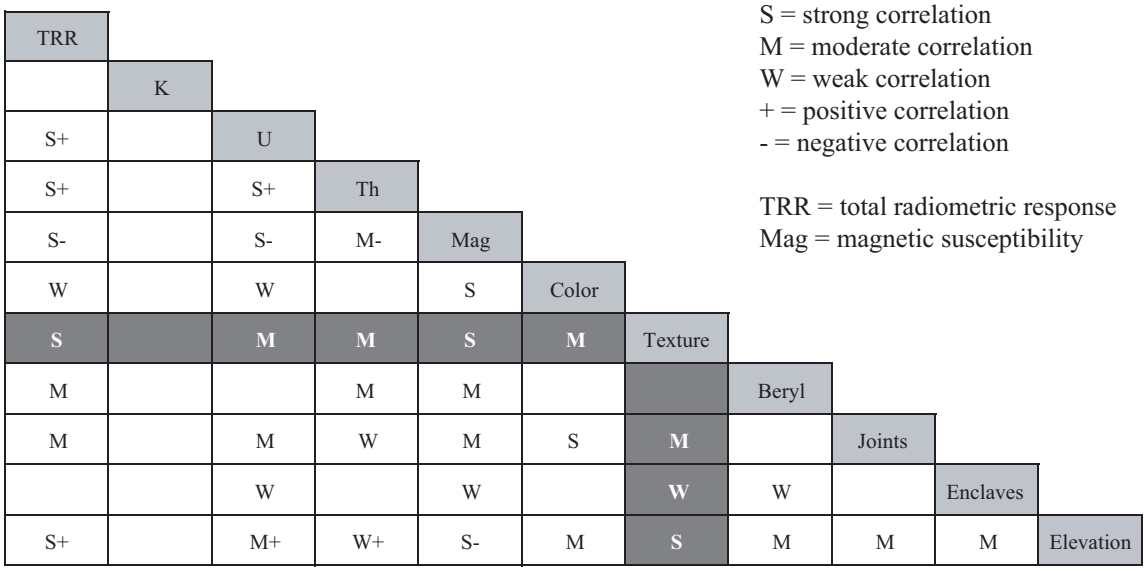

Figure 11. Chart summarizing correlations among variables in the Sheeprock Granite. To see correlations, chose a variable and trace its row and column as shown for texture.

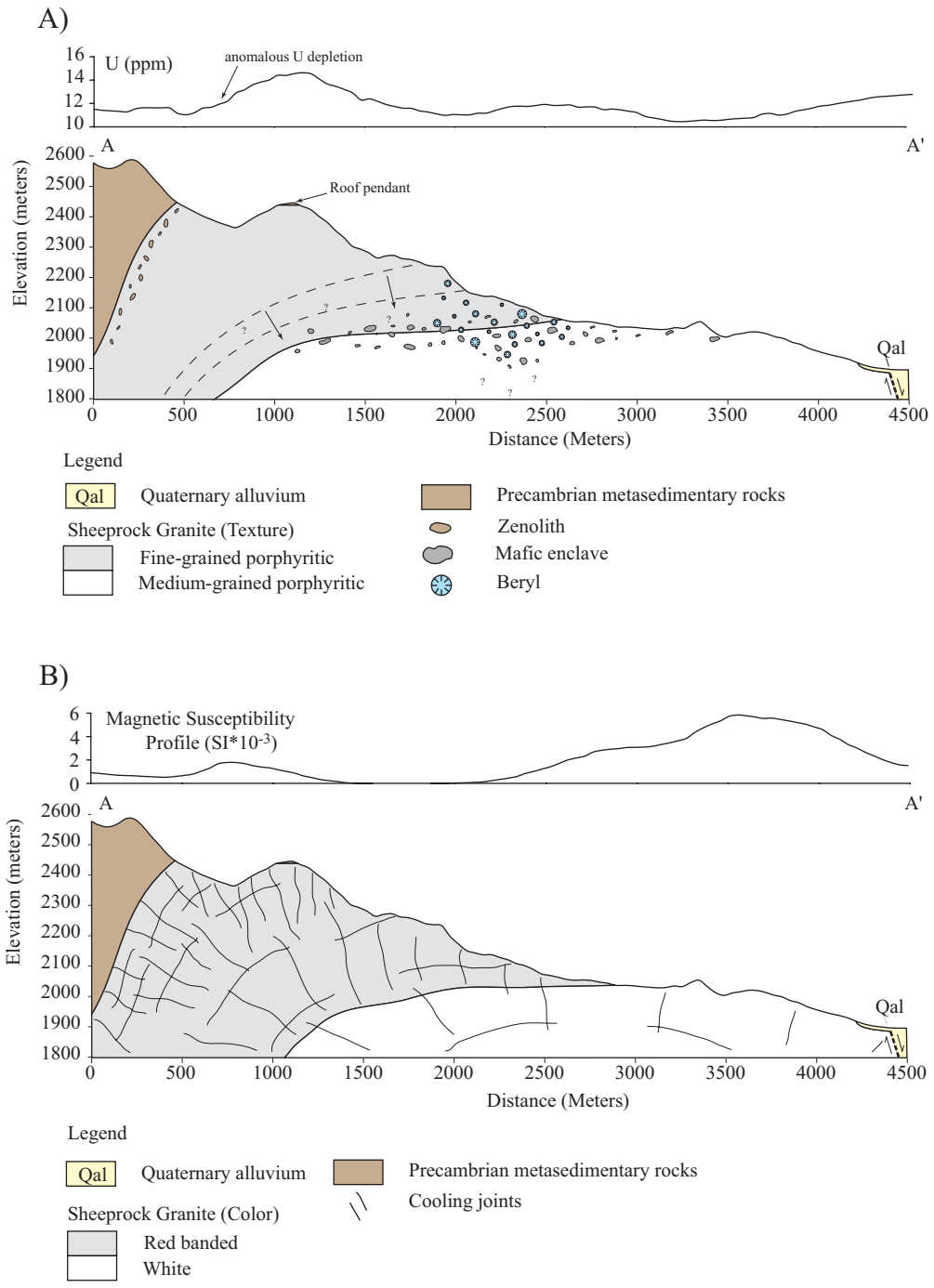

Figure 12. Cross-sections (along the A-A' line in Figure 1) of A) magmatic features including a uranium profile, and B) post-magmatic features including a profile of the magnetic susceptibility. Verticle exaggeration 2:1.

a concentric pattern of finer-grained granite along the margins to medium-grained granites in the center, we suggest the intrusion may have been truncated by a NW-trending normal fault, due to a lack of finer-grained textures along the southwestern margin. This is in agreement with Cohenour's (1959) "Western Flank" and "Southern Flank" fault zones. Uranium and thorium often behave as incompatible elements and are enriched in the more evolved parts of granitic intrusions (Rogers et al., 1978; Simpson, 1979; Webb et al., 1987; Thorpe et. al., 1995). In the case of the Sheeprock granite, very low concentrations of eU and eTh combined with enrichments in Fe, Mg, Ti and other compatible elements in rocks from the Copper Jack area may be evidence for an early pulse of less differentiated magma (or "mafic" cumulates crystallized from such a pulse). The rest of the pluton has higher concentrations of Th and especially U. Uranium and thorium are concentrated in the finer-grained rocks along the intrusive margin and less concentrated in the coarser-grained rocks in the core of the pluton (Figures 6c, d; 7b). This can be explained by the fractionation of uranium and thorium into accessory minerals that accumulated along the roof and walls of the second` stage of the intrusion. This wall crystallization would have depleted the residual melt in U and Th and displaced it inward (Bowden et al., 1981; Webb et al., 1987). Figure 13 shows Th and U against incompatible Rb. Notice how U and Th increase with differentiation and then decrease presumably because of fractionation of Th and U-rich accessory phases. Thus, Th and U are depleted in "Group 1" rocks in the core. Indeed, Funkhouser-Marlof (1985) found that uranium and thorium along the margins of the pluton are concentrated in uraninite, uranoan thorite, thorite, niobium-tanalum oxides, monazite, zircon, and

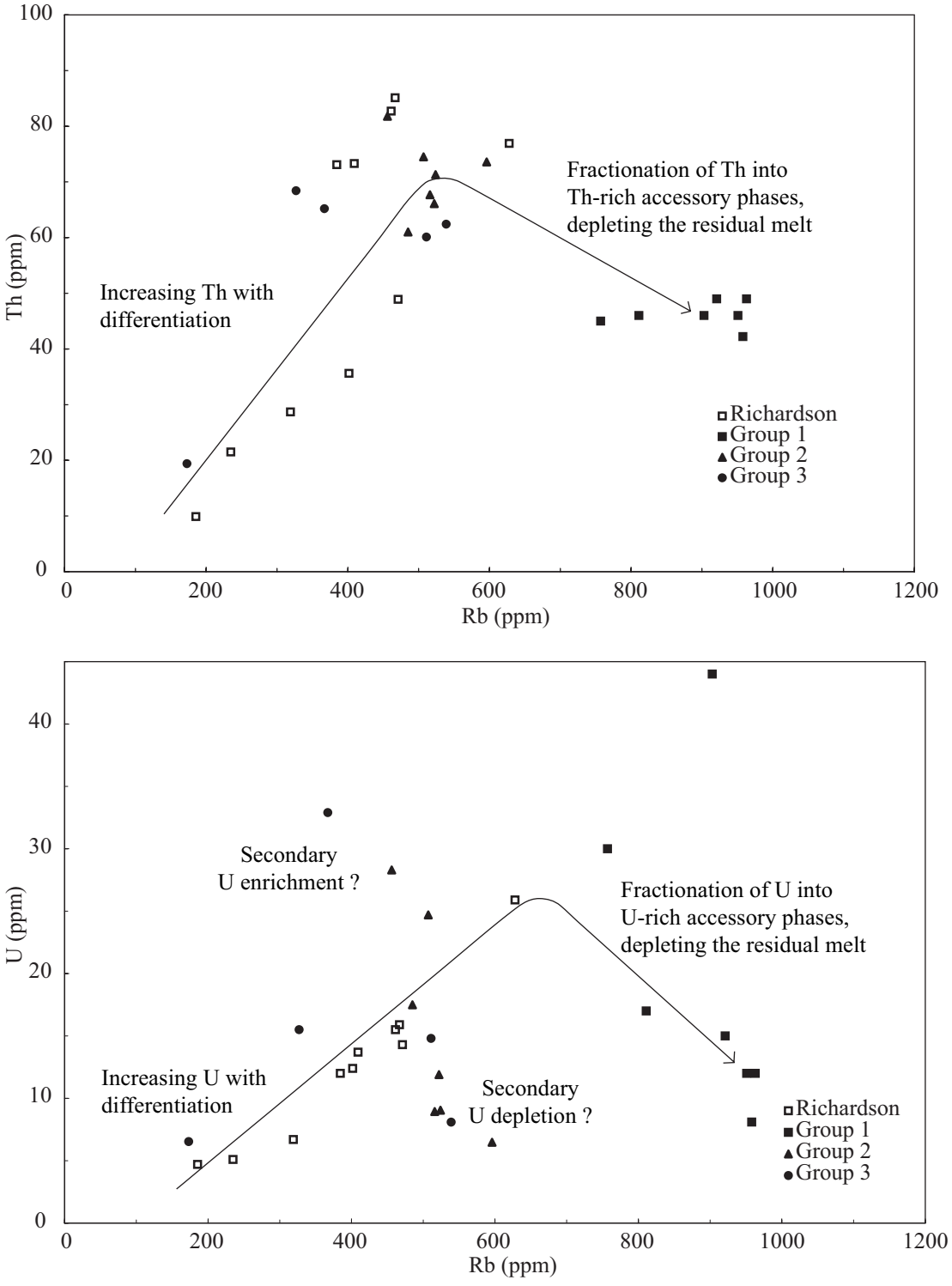

Figure 13. Th and U plotted against incompatible Rb. Initially, both Th and U increase with differentiation, until Th & U-rich accessory minerals begin to fractionate. Groups 1, 2, and 3 are from Christiansen et al. (1988).

allanite. Monazite and thorite are the most important sites for uranium and thorium in the radioelement enriched parts of the Sheeprock granite. This can be seen on the uranium map (Figure 6c) and uranium profile in Figure 12a. It appears intermediate concentrations of Th still remained in the more evolved (beryl bearing) portions of the pluton (Figures 6d, 7c).

Alternatively, low uranium concentrations (particularly in areas that have experienced greater degrees of alteration or weathering) could be the result of post-magmatic uranium mobilization (Funkhouser-Marloff, 1985; Wu, 1991). Uranium is relatively soluble in its oxidized hexavalent state and could have been leached from the granite during alteration and weathering. Scatter in U along the magmatic trend may be evidence of uranium enrichment and/or depletion (Figure 13). The low uranium "tongue" beginning in Hard to Beat canyon and extending to the northern slopes of Sheeprock canyon does not correlate with magmatic Th and may be the result of secondary mobilization. However, the overall similarities in the distributions of U and less soluble thorium suggest minimal remobilization and that the uranium distribution is primarily magmatic (Rogers et al., 1978; Nash, 1979). This implies secular disequilibrium in the ^{238}U series is not significant in the Sheeprock granite (Cassidy, 1981). In addition, the drop in uranium and thorium across the contact indicate they were not strongly affected by hydrothermal processes (Simpson, 1979).

The arcuate chemical patterns seen on maps of total radiometric response, U and Th suggest the granite was cut by faulting along its southwestern margin, which truncated a more concentric zonation. This supports existing fault evidence as discussed earlier in

the text.

The Th/U ratio can also be a key indicator of magmatic and post-magmatic processes. The wide variation in Th/U from 0.4 to 8.8 (Figure 4) can obviously be caused by variations in either element. The mean Th/U ratio for the Sheeprock granite (4.0 ± 1.7) is similar to that of fresh magmatic granites. The most evolved parts of the intrusion "Group 1" have Th/U ratios > 6 (Figure 7a). This could imply an increase in the Th/U ratio with differentiation, moderate Th enrichment in the core, or be evidence of late stage or secondary remobilization of uranium (Rogers et al., 1978; Stuckless, 1981). Figure 14 shows the Th/U ratio increasing with Th. Extremely high Th/U ratios (> 8) resulting from low U concentrations may be attributed to U depletion. In addition, the broad ragged peak on the histogram (Figure 5) and the patchy nature (of highs and lows) of this map (Figure 7a) may be further evidence for some secondary remobilization of uranium (Rogers et al., 1978).

Beryl concentrations are believed to represent the most differentiated portions of the pluton and were restricted to "group 1" of Christiansen et al. (1988; Figure 1). As the pluton cooled from the roof downward, incompatible elements (like Be) were displaced toward the center. Beryllium may have concentrated in two areas along the textural boundary or solidification front before the magma completely crystallized (Figure 7c, b). The rosettes may have formed rapidly by a sudden drop in pressure, possibly from fracturing in the magma chamber (Rogers, 1990; Knapp, 1981). This sudden drop in pressure may be related to the injection of a more mafic melt (i.e., mafic enclaves) and the formation of aplite dikes.

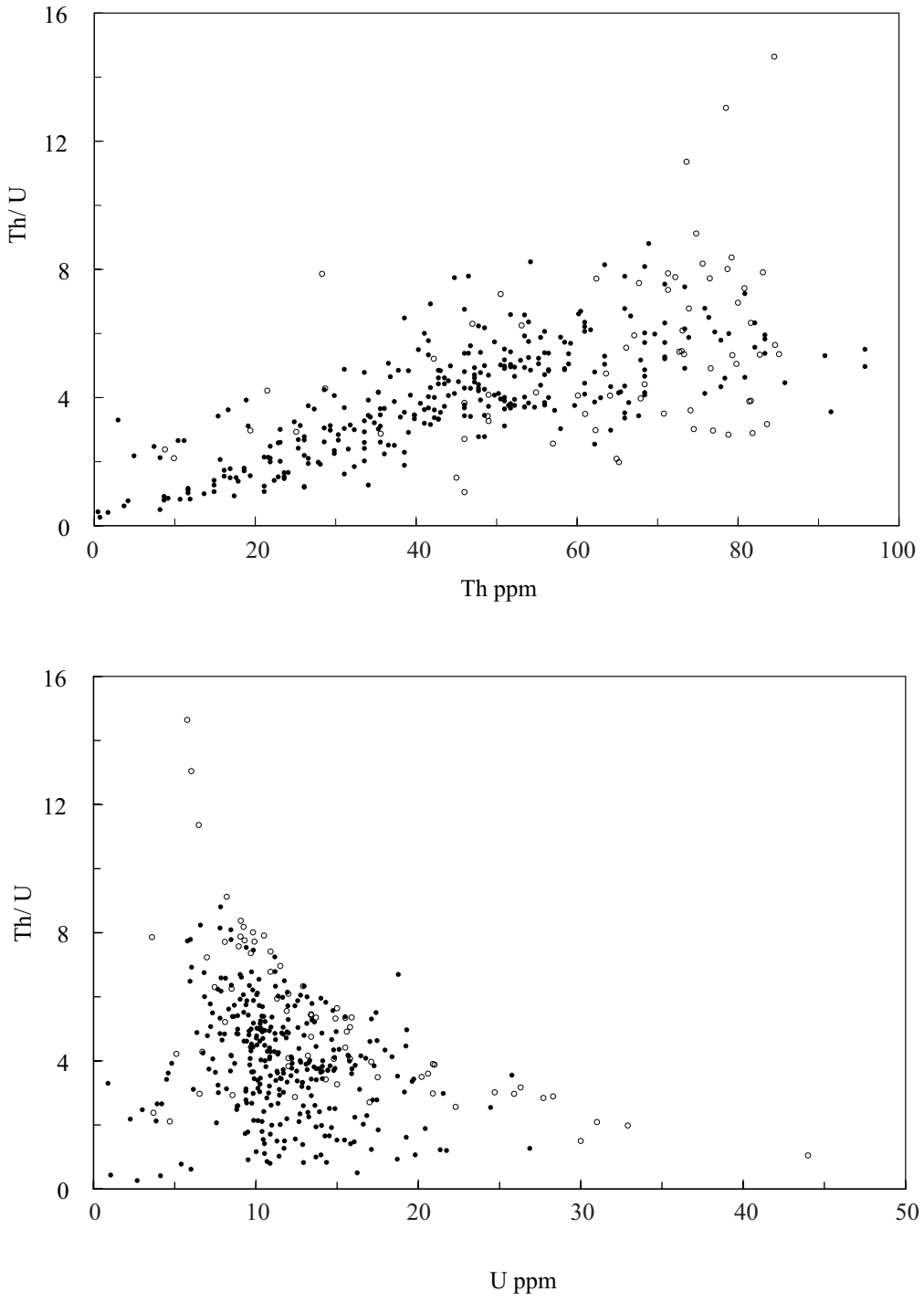

Figure 14. Includes U & Th variations in the Sheeprock granite. Whole rock analyses (open cirlces), and gamma-ray spectrometry data collected in the field (closed circles).

Though not the emphasis of this study, the NW-SE string of mafic enclaves generates more questions than answers. Possible origins for mafic enclaves include:

- injection of a less differentiated melt from deeper in the same chamber
- mafic injection from an unrelated source
- remobilization of early cumulates that formed along chamber walls
- reequilibrated / recrystallized xenoliths of metasedimentary country rock

The last of these possibilities seems less likely for the Sheeprock granite, because of the mafic nature of the enclaves compared to the Qtz-rich wall rocks. Moreover, subhedral titanite and epidote in conjunction with multiple morphologies of apatite are not likely to have originated from the country rock. Experimental studies have shown that smaller stubby apatite crystals form during equilibrium crystallization, whereas elongated prisms form during undercooling of magma (Didier, 1973). The two morphologic types of apatite may suggest enclaves were quenched during magma mixing and not just remelted remnants of country rock. Trace element patterns (Figure 10) show the enclave to be enriched in certain elements relative to the host granite and lacks a negative Nb anomaly. The lack of a negative Nb anomaly suggests these magmas may have originated from different sources. Mafic enclaves represent blebs of a less differentiated magma injected into the main, more felsic magma. The enclave melt invaded the crystallizing magma chamber after the formation of alkali feldspar phenocrysts, but before solidification of the groundmass, as seen in the enclaves of the Dinky Creek granite described by Dorais et al. (1990). Sharp contacts formed as the mafic magma quenched in the cooler granitic magma. It is possible that the quenching of these enclaves released enough volatiles and

increased H_2O pressures enough to fracture the already crystalline part of the intrusion, resulting in a sudden drop in pressure, spawning the formation of beryl rosettes.

Based on their general NW-SE trend (parallel to the orientation of the pluton, extension related faults, and microcracks related to paleostress fields), they may have been emplaced through the same dikes (feeder zone) that created the pluton (Cohenour, 1959; Kowallis et al., 1995). Alternatively, the mafic blebs may have encountered a downward propagating solidification front (marked by the transition from fine to medium-grained matrix), and spread laterally (Figure 7b, 12a). These enclaves are weakly restricted between the elevations of 1,950 and 2,250 meters (above sea level), similar to the beryl horizon described by Htay (1976). Bachl et al. (2001) describes a similar occurrence in the Searchlight pluton in which mafic enclaves are limited to certain horizons based on density and transition zones between crystal-rich and crystal-poor magmas.

Mafic enclaves found in the Sheeprock granite may be similar to mafic inclusions in the chemically and temporally comparable 21 Ma Spor Mountain rhyolite and linked to the bimodal magmatism of the time (Christiansen et al., 1990). However, due to slower rates of cooling and longer periods of chemical diffusion and hybridization between mafic and silicic melts, the original composition of these enclaves is far from clear. Further investigation is required to constrain this hypothesis.

Higher concentrations of aplite dikes in the medium-grained granite, suggest they likely originated from the more differentiated core regions (Figure 7b). These dikes may have formed by filling voids created when the chamber was fractured after the

introduction of the mafic enclave melt.

Post Magmatic Processes

Joint spacing appears to have played a major role in the post-magmatic evolution of the Sheeprock granite. Kowallis et al. (1995) concluded that microcracks in quartz formed as the granite cooled below about 350°C. Their orientations have a direct correlation to the paleostress field (parallel to the maximum horizontal stress) showing a preferred NW-SE orientation. However, larger joints failed to show this connection and were generally oriented N-S and thought to be the result of cooling, unroofing of the pluton, and later faulting.

To the extent that closer joint spacings are related to more rapid cooling and higher magma pressures (Knapp and Norton, 1981), a more dense concentration of joints should occur in areas of greater geothermal gradients (especially near the roof zone), while more widely spaced joints form at a distance from the margin. This has been demonstrated in starch-water mixture experiments in which joint density is inversely proportional to the cooling rate (Toramaru and Matsumoto, 2004; Grossenbacher and McDuffie, 1995). Our proposed model for joint formation is similar to that described by Kano and Tsuchiya (2000), where joint spacing in granite intrusions increases away from the margins toward the center due to differential cooling processes (Figure 12b). In the case of the Sheeprock granite, there are a limited number of areas with closely spaced joints (10 cm or less; Figure 8a). This may be because, areas with closely spaced joints are more easily weathered and eroded, exposing less dense jointing below them. It is proposed that areas having fewer joints (i.e., the white granite in the southwestern portion

of the pluton) are exposed because the more closely spaced joint sets that were once above them have been eroded away. Thus, granite with fewer joints may represent deeper parts of the magma chamber (Figure 12b).

Color patterns in the granite correlate well with joint spacing (Figure 8b and a). Most red-banded granite is in areas of higher joint density; while jointing in white granite is less dense. Harris (1957) also noted this correlation. Because joints control the flow of post-magmatic fluids (commonly cool oxidized meteoric groundwater), areas with more closely spaced joints experienced greater degrees of oxidation and alteration and consequently more weathering and erosion (Selby, 1980; Tsutsue and Ishihara, 1978). Granite with lower joint density (white granite) remains fresher and less oxidized (Ehlen, 1999). Color may also be controlled by magmatic processes; areas stained red may have greater amounts of iron-bearing minerals, while white areas have lower concentrations of mafic minerals. This agrees with more mafic cumulates forming along the margins displacing residual melts depleted in iron inward.

Magnetic susceptibility is a measure of the abundance of magnetite within a rock and in many cases is proportional to whole rock Fe content in fresh outcrops (Gleizes et al., 1993). Blevin (2003) was able to show a strong correlation between magnetic susceptibility and total Fe content based on his studies of I- and S-type granites in Australia. Gleizes et al. (1993) also mapped compositional zonation in ilmenite-series granitic rocks in the Mont-Louis Andorra Granite. According to Ishihara's two-fold classification, the least oxidized rocks in the Sheeprock pluton are low in the range for magnetite-series granites (3 to about $20*10^{-3}$ SI units) as compared to ilmenite-series

granites (less than $3*10^{-3}$ SI units; Ishihara, 1977). Dall'Agnol's (in press) studies of A-type Brazilian granites, have identified a possible intermediate series ranging from 3 to 10 SI$*10^{-3}$, similar to that of the Sheeprock granite. Magnetite series granies are characteristic of I- and A-type granites (Gregorova et al., 2003). The positive correlation between magnetic susceptibility and Fe_2O_3 concentration is consistent with the magnetite controlling the magnetic susceptibility of fresh rocks (Figure 9). The highest magnetic susceptibility in the pluton occurs in the southeastern corner around Copper Jack mine ($10.7*10^{-3}$ SI). Modal mineralogy (~ 5% mafic minerals) and whole rock compositions show this area to be the most mafic part of the pluton (Table 1, sample CJ). This area may represent an early mafic pulse (or mafic cumulate phase as interpreted by Christiansen et al., (1988) that was later intruded by the main body of the intrusion. This interpretation is also supported by its low Th and U concentrations and distinctive trace element pattern (Figure 10). A small magnetic high near the northeastern contact seen on Figure 12a, may be evidence that some mafic cumulates formed along the margins of the pluton and escaped oxidation because of relatively low joint density.

However, the bimodal distribution of magnetic susceptibility in the Sheeprock granite (Figure 5) suggests post-magmatic processes have been effective. Magnetic susceptibilities ranging from 0.01 to $0.34*10^{-3}$ SI with a low mode of ~$0.07*10^{-3}$ SI represent rocks in which magnetite has been oxidized or destroyed, while susceptibilities ranging from 0.36 to $12.7*10^{-3}$ SI with a mode of ~ $5.4*10^{-3}$ SI represent less oxidized rock. Figure 9 shows total iron vs. magnetic susceptibility, where the expected variation trend is based on data collected by Blevin (2003) for I-type granites. Points that fall to

the left of the expected variation have been oxidized. Magnetite in areas of low susceptibility has been altered to limonite or hematite as evidenced by the strong correlation between reddish-brown staining and low magnetic susceptibility (Figures 8c and b). Moreover, this alteration is most prevalent in areas of greater joint density (Figure 8a). Magnetite in areas where joints are spaced farther apart, tends to be less altered by oxidizing fluids and the granite is white. Studies conducted by D. Kimbrough of San Diego State University (written communication, 2004) also concluded in-situ weathering of plutonic rock can significantly reduce its magnetic susceptibility due to oxidation of magnetite.

The apparent correlation between greisen and low Th concentrations along the northeastern portion of the pluton is interesting (Figures 6c; 7b). It is possible that Th was preferentially leached out by post-magmatic fluids and deposited in greisen. Preliminary studies showed greisen to be enriched up to 100% in K_2O, eU, and eTh relative to the host granite. Greisen may represent conduits for post-magmatic remobilization of radioelements.

ORIGIN OF SHEEPROCK GRANITE ZONATION

From the results of this study a more thorough picture of the magmatic and post-magmatic evolution of this pluton can be constructed.

Magmatic Processes

The emplacement and differentiation of the Sheeprock granite can be summarized in 6 stages (Figure 15).

Stage 1. Initial magmatism is represented by rocks found only in the Copper Jack

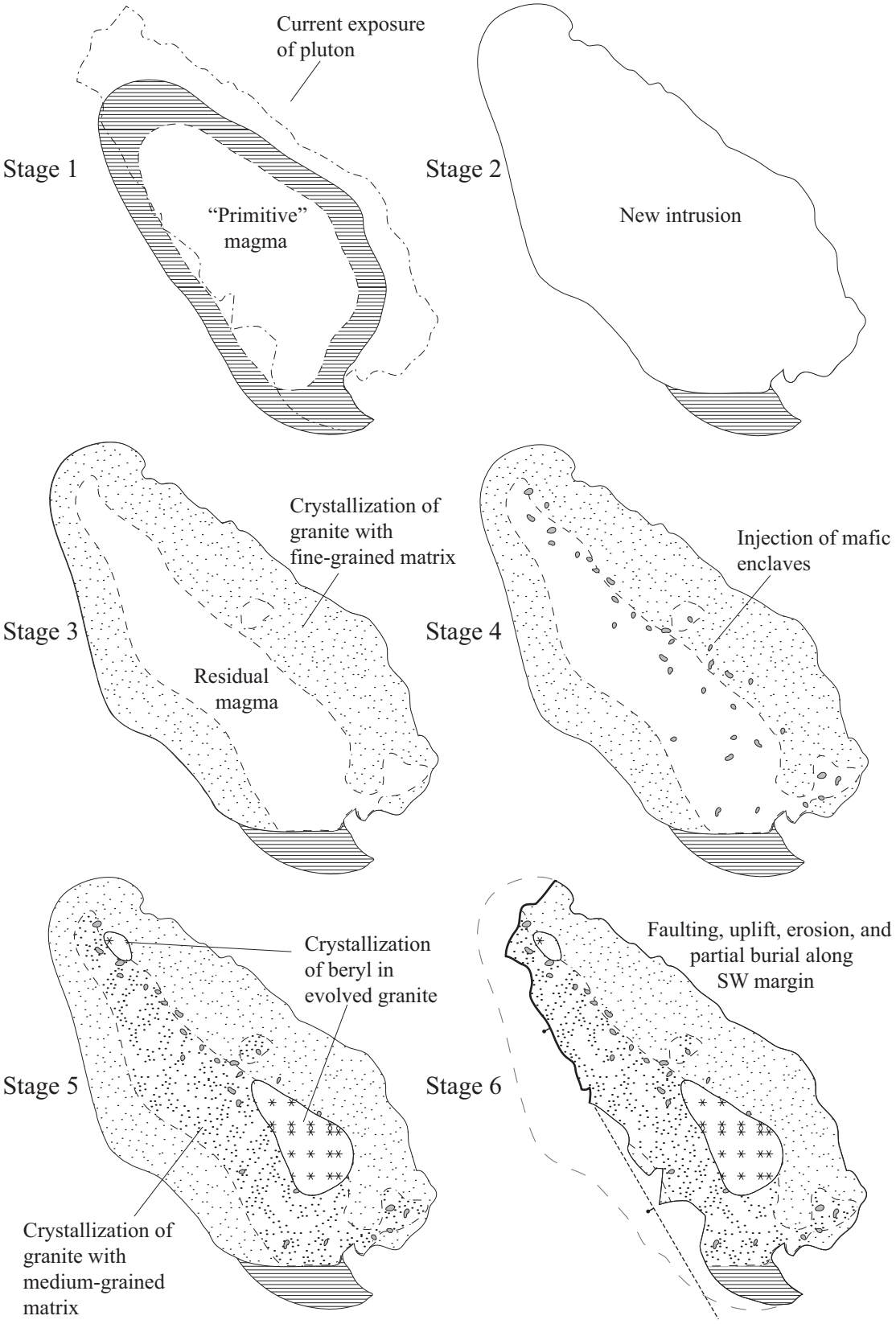

Figure 15. Emplacement and development of the Sheeprock Granite, shown in map view.

mine area. They are probably early cumulates and consequently are depleted in U and Th and have mafic compositions. Magma possibly intruded along a NW-SE oriented dike or fault, parallel to the maximum horizontal stress 21 million years ago, giving the pluton its elliptical shape (Cohenour, 1959; Blatter, 1992).

Stage 2. A second pulse of the same magma intruded upward consuming most of the original intrusion except for the southeastern tip, entraining xenoliths of country rock along the margins.

Stage 3. Porphyries with fine-grained matrices formed along the roof and walls as the magma crystallized creating a inward-propagating crystallization front. U and Th are fractionated into accessory monazite and thorite that accumulated along the margins and depleted the residual liquid which was displaced inward. Incompatible elements like F, Be, and Rb were strongly enriched in the residual core melt.

Stage 4. A third pulse of mafic magma (possibly related to bimodal volcanism of the time) intruded and was disaggregated along the crystallization front. Enclaves incorporated phenocrysts of K-feldspar from the granitic magma and were quenched and partially equilibrated with the surrounding melt. This quenching may have been a catalyst increasing volatile pressure enough to fracture the chamber and drop pressures inducing the crystallization of beryl rosettes.

Stage 5. Continued solidification produces medium-grained matrix textures formed away from the margins, up to 1 kilometer from the contact, due to slower cooling rates. Crystallization of beryl along the solidification front in the highly differentiated core of the pluton represents the final stage of solidification. Small crystals of blue beryl

formed, some of which served as seeds for the development of larger rosettes. Beryl is concentrated in two zones which may represent two separate centers of Be-rich residual melt accumulation. Water-rich residual liquids escaped through fractures (possibly tied to the injection of mafic enclaves and rising water pressures) and early joints to form aplite dikes.

Stage 6. The current exposure of the pluton is the result of basin and range normal faulting and uplift that divided the granite, exposing part of it in the footwall of the Sheeprock horst. Weathering and erosion shaped the pluton as we see it today. Much of the southwestern corner is buried by alluvium.

Post-Magmatic Processes

Much of the Sheeprock granite's post-magmatic history can be interpreted from observations of joint spacing, color, and magnetic susceptibility (Figure 12b), and can be summarized in 3 phases.

Phase 1. After solidification microcracks and joints formed from cooling, tensile tectonic forces, and unloading. Jointing was most intense where temperature gradients were highest, along the roof and margins, and decreased away from the intrusive contact.

Phase 2. Joints served as conduits for fluids promoting alteration, oxidation, and eventually weathering and erosion. Greisenization occurred along these joints in areas of moderate to high joint density. Areas of high joint densities are prone to erosion and are rarely preserved, except along the intrusive margin.

Phase 3. Iron-bearing minerals such as magnetite and pyrite were oxidized to hematite and limonite by these fluids creating a reddish stain and the banded appearance

of much of the granite. The destruction of magnetite lowered magnetic susceptibilities and is most noticeable in areas of intense jointing and red staining.

SUMMARY

Field gamma-ray spectrometry, magnetic susceptibility measurements and simple observations (e.g., color, texture and joint spacing) provide a quick and affordable method for assessing zoning patterns in granitic plutons. This approach is useful in creating preliminary models of magmatic and post-magmatic processes, prompting new questions, and guiding the collection of samples for detailed lab analysis.

The use of a global positioning system (GPS) combined with a geographic information system (GIS) proved a very effective way to collect and manage these data. Spatial analysis of data allowed us to see and interpret physical and chemical patterns not apparent in the field.

Our results show high concentrations of U and Th along much of the intrusive contact, suggesting the formation of U and Th-rich cumulates along pluton margins. In addition, texture, joint spacing, and magnetic susceptibility were useful in characterizing the zonation of the pluton, and supported evidence of in situ crystal fractionation from the roof down and from the walls inward. The possibility of a preserved solidification front marked by the transition from fine to medium-grained matrix textures may have played a role in the distribution of mafic enclaves and beryl. Magnetic susceptibility is bimodal. The low mode reflects the oxidation of magnetite (responsible for the red staining) and the high mode is representative of fresh (less oxidized) rock and is at the low end of magnetite-series granites. Post-magmatic oxidation of magnetite was

controlled by joint density and was greatest in areas having closer joint spacings.

From this study we were able to answer many of our initial questions regarding the formation of the Sheeprock pluton and its physical and chemical variations. Patterns in U and Th concentrations suggest an asymmetrical zonation and support evidence of range front faulting. There are no discernable significant internal contacts; however, when spatially analyzed boundaries between chemistry, texture, joint density, and color can be identified. Boundaries are for the most part gradational; nevertheless, as seen in the area of Copper Jack mine they can have steep gradients, and may correlate with intrusive episodes. Some variations are patchy as in Th/U. Chemical and textural evidence supports in-situ crystallization from the margins inward. The Sheeprock granite is composed of at least 3 magma pulses. The initial pulse, represented by granite in the Copper Jack area, is the most mafic and may be cumulate in nature. The second pulse makes up the rest of the granite and is concentrically zoned. The late injection of a mafic magma responsible for the enclaves is represented in the third phase.

In the case of the Sheeprock granite, field results agreed well with previous lab-based geochemical whole rock data, but dramatically expanded our understanding of the pluton's zonation and cooling history. Because of the density and distribution of field measurements made over the pluton, a more complete/realistic map of elemental concentrations could be made.

REFERENCES

Bachl, C.A., Miller C.F., Miller J.S., and Faulds, J.E., 2001, Construction of a pluton: Evidence from an exposed cross section of the Searchlight pluton, Eldorado Mountains, Nevada: Geological Society of America Bulletin, v. 113, p. 1213-1228.

Blatter, T.K., 1992, Fracture orientations in granitic rocks as indicators of regional paleostress within the Eastern Great Basin and Range Province, Utah: M. S. Thesis, Brigham Young University, p. 38.

Blevin, P.L., 2003, Metallogeny of Granitic Rocks: Australian Geological Survey Organization, The Ishihara Symposium: Granites and Associated Metallogenesis, Abstract, p. 1-4.

Bowden, P., Bennett, J.N., and Kinnaird, J.A., 1981, Uranium in the Niger-Nigeria Younger Granite Province: Mineralogical Magazine, v. 44. p. 379-389.

Cassidy, J., 1981, Techniques of field gamma-ray spectrometry: Mineralogical Magazine, v. 44, p. 391-398.

Chiozzi, P., Pasquale, V., and Verdoya, M., 1998, Ground radiometric survey of U, Th and K on the Lipari Island, Italy: Journal of Applied Geophysics, v. 38, p. 209-217.

Christiansen, E.H., Stuckless, J.S., Funkhouser-Marlof, M.J., and Howell, K. H., 1988, Petrogenesis of rare-metal granites from depleted crustal sources: An example from the Cenozoic of western Utah, U.S.A.: CIM special Publication 39, p. 307-321.

Christiansen, E.H,. and Venchiarutti, D.A., 1990, Magmatic inclusions in rhyolites of the Spor Mountain Formation, western Utah; Limitations on compositional inferences from inclusions in granitic rocks: Journal of Geophysical Research, v. 95, p. 17,717-17,728.

Cohenour, R., 1959, Sheeprock Mountains, Tooele and Juab Counties, Precambrian and Paleozoic stratigraphy, igneous rocks, structure, geomorphology and economic geology: Utah Geological and Mineral Survey Bulletin, v. 63, 201 p.

Dall'Agnol, R., Oliveira, D., 2004, Oxidized rapakivi-type granites of Carajás, Brazil: A-type or I-type?: Goldschmidt conference, Copenhagen, Denmark, p. A674, abstract, in press.

Didier, J., 1973, Granites and their Enclaves, The bearing of enclaves on the origin of granites: Elsevier Scientific Publishing Company, Amsterdam, London, Developments in petrology, v. 3, p. 239-240.

Dorais, M.J., Whitney, J.A., Roden, M.F., 1990, Origin of Mafic Enclaves in the Dinkey Creek Pluton, Central Sierra Nevada Batholith, California: Journal of Petrology, v. 31, p. 853 - 881.

Ehlen, J., 1999, Fracture characteristics in weathered granites: Geomorphology, Elsevier Science, v. 31, p. 29-45.

Funkhouser-Marlof, M.J., 1985, The mineralogy and distribution of uranium and thorium in the Sheeprock Granite, Utah: M. S. Thesis, University of Iowa, 60 p.

Gleizes, G., Nedelec, A., and Bouchez, J., 1993, Magnetic Susceptibility of the Mont-Louis Andorra Ilmentite-Type Granite (Pyrenees): A New Tool for the Petrographic Characterization and regional mapping of Zoned Granite Plutons: Journal of Geophysical Research, v. 98, p. 4317-4331.

Gregorova, D., Hrouda, F., and Kohut M., 2003, Magnetic susceptibility and geochemistry of Variscan West Carpathian granites: implications for tectonic setting: Physics and Chemistry of the Earth, v. 28, p. 729-734.

Grossenbacher, K.A., and McDuffie, S.M., 1995, Conductive cooling of lava: Columnar joint diameter and stria width as functions of cooling rate and thermal gradient: Journal of Volcanology and Geothermal Research, v. 69, p. 95-103.

Harris, D., 1957, The Geology of Dutch Peak Area, Sheeprock Range, Tooele County, Utah: M. S. Thesis, Brigham Young University, p. 82.

Htay, H., 1976, Geology and geochemistry of beryllium, tin and tungsten in granite area, Sheeprock Mountains, Toole and Juab Counties, Utah: unpublished manuscript.

Ishihara, S., 1977: The magnetite-series and ilmenite-series granitic rocks: Mining Geology, Japan, v. 27, p. 293–305.

Kano, S., and Tsuchiya, N., 2000, Parallelepiped cooling joint anisotropy of P-wave velocity in the Takidani granitoid, Japan Alps: Journal of Volcanology and Geothermal Research, v. 114, p. 465-477.

Knapp, R.B., and Norton, D.L., 1981, Preliminary numerical analysis of processes related

to magma crystallization and stress evaluation in cooling pluton environments: American Journal of Science, v. 281, p. 35-68.

Kowalis, B.J., Christiansen, E.H., Blatter, T.K., and Keith, J.D., 1995, Tertiary paleostress variation in time and space near the eastern margin of the Basin and Range province, Utah: Rossmanith (ed.), Mechanics of Jointed and Faulted Rock: Rotterdam: Balkema, p. 297-302.

McDonough, W.F., and Sun, S.S., 1995, Chemical Evolution of the Mantle: Chemical Geology, v. 120, p. 223-253.

Nash, J.T., 1979, Uranium and thorium in granitic rocks of northeastern Washington and northern Idaho, with comments on uranium resource favorability: Open-File Report 79-233, U.S. Geological Survey, 46 p.

Pampeyan, E.H., 1989, Geologic Map of the Lynndyl 30- by 60-Minute Quadrange, West-Central Utah: Miscellaneous Investigation Series G, U.S. Geological Survey, 1:100,000 scale, map I-1830.

Peterman, Z.E., Bunker, C.M., Snyder, G.L., and Bush, C.A., 1981, U, Th, and K contents of some major Precambrian lithologic units of the Hartville Uplift, Wyoming: Open-File Report, U.S. Geological Survey, 16 p.

Phair, G., and Gottfried, D., 1964, The Colorado Front Range, Colorado, U.S.A., as a uranium and thorium province, in the National Radiation Environment: University of Chicago Press, p. 7-38.

Pitcher, W.S., 1982, Granite type and tectonic environment: In, Hsu, K. J. *ed*., Mountain building processes: Academic press, London, p. 19-40.

Rogers, J.J., Ragland, P.C., Nishimori, R.K., Greenberg, J.K., and Hauck, S.A., 1978, Varieties of granitic uranium deposits and favorable exploration areas in the eastern United States: Economic Geology, v. 73, p. 1539-1555.

Rogers, J.R., 1990, Origin of beryl in the Miocene Sheeprock granite, west-central Utah: M. S. thesis, Brigham Young University, 48 p.

Selby, M.J., 1980, A rock mass strength classification for geomorphic purposes: with tests from Antarctica and New Zealand: Zeitschrift fuer Geomorphologie, v. 24, p. 31-51.

Simpson, P.R., 1979, Uranium mineralization and granite magmatism in the British Isles: Philosophical Transactions of the Royal Society of London, Series A: Mathematical and Physical Sciences, v. 291, p. 385-412.

Stuckless, J.S., Bunker, C.M., Bush, C.A., and Van Trump, G. Jr., 1981, Radioelement Concentrations in Archean Granites of Central Wyoming, Open-File Report 81-948, U.S. Geological Survey, 40 p.

Stuckless, J.S., and Van Trump, Jr.G., 1982, A compilation of radioelement concentrations in granitic rocks of the contiguous United States: U.S. Geological Survey, p. 191-208.

Thorpe, R.S., Tindle, A.G., and Williams-Thorpe, O., 1995, Radioelement distribution in the Tertiary Lundy granite (Bristol Channel, UK): Geology Magazine, v. 132, p. 413-425.

Toramaru, A., and Matsumoto, T., 2004, Columnar joint morphology and cooling rate: A starch-water mixture experiment: Journal of Geophysical Research, v. 109, DOI: 10.1029/2003JB002686, 10 p.

Tsutsue, A., Ishihara, S., 1978, Degree of oxidation of the granitic magmas in the molybdenum, tungsten, and tin provinces of Southwest Japan: Metallization Associated with Acid Magmatism, Geological Survey of Japan, v. 3, p. 305-311.

Webb, P.C., Tindle, A.G., and Barritt, S.D., 1987, Factors controlling the distribution of heat production in selected UK granites: Geophysical Research Letters, v. 14, p. 299-302.

Whitney, J.A., 1975, The effects of pressure, temperature, and X_{H2O} on phase assemblages in four synthetic rock compositions: Journal of Geology, v. 83, p. 1-27.

Wu, L., 1991, Greisenization of the Sheeprock Granite, west-central Utah: A fluid inclusion and geochemical study: M. S. Thesis, Brigham Young University, 41 p.

APPENDIX A

MAP PROPERTIES

Total radiometric response (cps)
Method: Simple Kriging
Number of Points: 521
Neighbors: 2-5 for each angular sector
Angular Sectors: 4
Classification: Smart Quantile

K_2O (wt%)
Method: Simple Kriging
Number of Points: 527
Neighbors: 2-5 for each angular sector
Angular Sectors: 4
Classification: Smart Quantile

eU (ppm)
Method: Simple Kriging
Number of Points: 527
Neighbors: 2-5 for each angular sector
Angular Sectors: 4
Classification: Smart Quantile

eTh (ppm)
Method: Simple Kriging
Number of Points: 308
Neighbors: 2-5 for each angular sector
Angular Sectors: 4
Classification: Smart Quantile

Th/U ratio
Method: Simple Kriging
Number of Points: 308
Neighbors: 2-5 for each angular sector
Angular Sectors: 4
Classification: Manual

Texture

Method:	Simple Kriging
Number of Points:	466
Neighbors:	2-5 for each angular sector
Angular Sectors:	1
Classification:	Manual

Elevation

Method:	Contoured Digital Elevation Model (DEM)
Number of Points:	n/a
Neighbors:	n/a
Angular Sectors:	n/a
Classification:	Equal Interval

Joint spacing

Method:	Universal Kriging
Number of Points:	472
Neighbors:	2-5 for each angular sector
Angular Sectors:	1
Classification:	Manual

Color

Method:	Universal Kriging
Number of Points:	517
Neighbors:	2-5 for each angular sector
Angular Sectors:	1
Classification:	Manual

Magnetic susceptibility ($SI*10^{-3}$)

Method:	Simple Kriging
Transformation:	Log
Number of Points:	523
Neighbors:	2-5 for each angular sector
Angular Sectors:	4
Classification:	Equal Interval

APPENDIX **B**

EXAMPLE OF SHEEPROCK DATA DICTIONARY

1. Point descriptions (point features)
    a. Tc2 (total radiometric response) cps
    b. K cps
    c. U cps
    d. Th cps
    e. Mag correction factor
        i. 1-10 mm in unevenness (no more than 5 mm is acceptable) default = 0
    f. Mag susceptibility - SI units
    g. Texture
        i. Fine-grained equigranular
        ii. Medium-grained equigranular
        iii. Coarse-grained equigranular
        iv. Fine-medium-grained seriate
        v. Medium-coarse-grained seriate
        vi. Fine-coarse-grained seriate
        vii. Fine-grained porphyritic
        viii. Medium-grained porphyritic
        ix. Coarse-grained porphyritic
    h. Miarolitic cavities
        i. 0 = no, default
        ii. 1 = yes
    i. Beryl
        i. 0 = no, default
        ii. 1 = disseminated crystals
        iii. 2 = rosette
    j. Color
        i. 0 = can't tell, default
        ii. 1 = red
        iii. 2 = white
        iv. 3 = banded
    k. Joint spacing
        i. 0 = none, default
        ii. 1 = 1 cm
        iii. 2 = 10 cm
        iv. 3 = 1 meter
        v. 4 = greater than 1 meter
    l. Dikes, greisen and veins
        i. 0 = none, default
        ii. 1 = dike

iii. 2 = greisen
iv. 3 = quartz vein
v. 4 = pegmatite
vi. 5 = rhyolite dike

m. Zenoliths and enclave types
i. 0 = ?
ii. 1 = mafic enclave
iii. 2 = quartzite
iv. 3 = metasedimentary
v. 4 = none, default

n. Zenolith and enclave sizes
i. 0 = none, default
ii. 1 = fist size or less
iii. 2 = greater than fist size

o. Notes

p. Sample #

q. Photo #

r. Time

s. Date

t. Contact (line feature)

u. Springs

v. Mines
i. Name of mine

APPENDIX C

TIPS TO A SUCCESSFUL RADIOMETRIC SURVEY

1. Instruments
   a. Care
      i. Read all manuals
      ii. Know how to troubleshoot minor problems in the field
      iii. Carry spare batteries or a way to charge your batteries in the field (e.g., a DC to AC power inverter that works off your car battery)
   b. Calibration and Statistics
      i. Follow all calibration procedures before using in the field.
         (1) The magnetic susceptibility meter does not require calibration.
         (2) Try to compare your values with someone else's values.
      ii. Choose a control point to measure at the beginning and end of each day.
         (1) Preferably in your field area
            (a) This is useful for determining the reproducibility of your data (precision). If it is not possible to determine precision prior to going to your field area repeated measurements on a slab of granite can help you determine instrument precision.
            (b) Recalibrate your gamma-ray spectrometer instrument every hour if possible to correct for instrument drift, detector decay, and or temperature changes. Record in your notes the timing of each calibration. Also calibrate at the beginning of each day.
      iii. Collect hand samples to analyze the whole rock chemistry
            (a) This will be used in comparing the manufacturer's conversions from cps to ppm and wt% for accuracy. It can also be used to calculate your own calibration line using linear and multi-linear regression techniques.
      iv. Statistics
         (1) Each measurement should be an average of several measurements to get the best representation of the rock. This will save you time and improve your counting statistics.
            (a) Use a running average to determine the minimum number of measurements needed at each point to best represent each outcrop.

c. Gamma-ray spectrometer
    i. Find a suitable place to measure
        (1) Find the largest, flattest, most unaltered out crops possible.
        (2) Place the instrument directly on the rock (keep it in the leather protective case)
        (3) Avoid measuring next to vertical faces; they will influence your results.
        (4) Record in the ten-second mode (tc2) for improved statistics.
        (5) Reduce the data each day. Check to see if it makes sense. Don't wait until the end of the field season to reduce the data.

d. Magnetic susceptibility
    i. Find a suitable place to measure
        (1) If the site is good enough for the gamma-ray spectrometer it will work for the magnetic susceptibility meter.
        (2) Surface unevenness
            (a) Each time you record a reading, include a surface correction factor. Correction values vary by instrument, but record the surface unevenness which is the distance between the sensor and the deepest pock mark. Anything less than 5 mm is acceptable.
        (3) Do not place the instrument near anything electrical as this will distort or even nullify your measurement. For example, calculator, GPS, cell phone, etc.
        (4) Measure several different places on the rock and average them to get a representative reading of that rock.

e. Data Collection
    i. Global Positioning System (GPS)
        (1) Data can be recorded in a number of ways; it is best to use a GPS system that can store data, but use a field notebook also.
        (2) GPS configurations can be adjusted beforehand to save time and make the transition from field data to a GIS system easier.
            (a) Change the GPS configurations to match the projections of the DEM(s), DRG(s), DOQ(s). The most common projections are NAD27 and NAD83.
            (b) Make all adjustments such as elevation in feet or meters, time zone changes, etc. prior to using in the field. However, these can be corrected using the "Pathfinder Office" program later if necessary.
            (c) Record location readings in UTMs

ii. Data Dictionary
(1) Using "Pathfinder Office" create a data dictionary to store and organize data collected in the field.
(a) Carefully organize field and attribute data in the order you will collect them in the field.
(b) With each field include a date and time attribute. This is a good way to organize your data and will be useful when you need to find a specific point in your notes.
(c) A copy of the data dictionary used for this survey is in Appendix B.

2. Fieldwork
a. Depending on how far you have to travel it is recommended you stay in your area several days at a time. This helps to save gas.
b. Encourage an undergraduate student to come along for invaluable experience. Have them carry some of your gear. Hiking with a partner is also a good thing to do from a safety perspective.
c. During the summer months, start earlier in the morning when it's cooler outside. Plan where you want to go the day before on a topographic map or aerial photograph.

3. Sample Collection
a. Select an outcrop to collect a handsample (1 to 2 lbs). First, measure it with the gamma-ray spectrometer and magnetic susceptibility meter, then collect your sample. This way you have the two values to compare with each other.
b. Collect at least 10 samples representing outcrops having a range of radioelement and magnetic susceptibility values.

4. Data Analysis
a. Before importing GPS data into ArcMap examine the data in Excel and make conversions from cps to ppm and wt%. You can also plot a number of graphs to identify outliers or questionable data.
b. Use ArcMap to perform various statistical analyses of your data. Determine which interpolation method works best for your data (e.g., kriging, inverse distance weighting, etc.).
i. We used a simple kriging model because it helps to smooth sporadic highs and lows, but was a good representation of our data.
c. Understand you will never be an Arcmap expert and will probably have to recreate your project several times. Become familiar with the help function and the ESRI online support website.

5. Data Interpretation
a. Rely on previous research and the guidance of peers to draw conclusions and correlations between chemistry and other field observations.

APPENDIX D

AREAS OF ADDITIONAL STUDY IN THE SHEEPROCK GRANITE,

WESTERN, UTAH

Over the course of this project new questions were generated that require additional study.

1. Is there any relationship between granite clasts found in Precambrian diamictites and the Sheeprock granite? Could it be a possible source rock for the Sheeprock granite?

2. What effect have meteoric and magmatic fluids played in the alteration and oxidation of the Sheeprock granite? Oxygen and hydrogen isotope work needs to be done.

3. Several large greisen (> 1 ft in width) were found between Hard to Beat and Cottonwood canyons and could be studied more thoroughly. Do they act as conduits for late removal of U and Th?

4. Though not mapped previously there is evidence for faulting along the northwestern contact of the pluton. Further investigations maybe able to prove this further as well as a continuation of that fault system to the south. A gravity and magnetic profile maybe useful in delineating this fault or determining the extent of the granite covered by alluvium.

5. More work needs to be done to better constrain the joint model, which would include multi-dimensional orientations of joints, density analyses, length of joints, and measurements of joint apertures.

6. A more detailed look at the origin and geochemistry of mafic enclaves would be useful in determining any relationships to enclaves found in contemporaneous volcanic rocks and to see if they are related to the Sheeprock granite.

7. Granite in the Copper Jack mine area is anomalous and has a very different signature that the rest of the pluton. This has been explained as a primitive melt of the Sheeprock granite, but further studies are needed to confirm this.

8. Further work can be done to demonstrate the correlation between magnetic susceptibility and total iron content in the Sheeprock granite, also the effects of weathering and alteration on the oxidation of magnetite.